EVALUATION OF SLURRY INJECTION FOR THE DETERMINATION OF METALS IN SOLID SAMPLES USING INDUCTIVELY COUPLED PLASMA ATOMIC EMISSION SPECTROMETRY

by

Ward-Mnaya J. Mavura

Dissertation submitted to the Faculty of the Virginia Polytechnic Institute and State University in partial fulfillment of the requirement for the degree of

Doctor of Philosophy

in

Chemistry

APPROVED:

Gary L. Long, Chairman

Mark R. Anderson

Larry T. Taylor

John G. Dillard

George Sanzone

August 1994
Blacksburg, Virginia

EVALUATION OF SLURRY INJECTION FOR THE DETERMINATION OF METALS IN SOLID SAMPLES USING INDUCTIVELY COUPLED PLASMA ATOMIC EMISSION SPECTROMETRY

by

Ward M. J. Mavura

Committee Chairman: Dr. Gary L. Long
Chemistry

ABSTRACT

It has been said that inductively coupled plasma (ICP) is the panacea for the determination of metals in environmental samples. The ease of sample introduction for liquids coupled with excellent limits of detection of this spectrometric method provide the analyst with the ability to perform rapid, multi-element determination of most elements in the periodic chart. However, when samples have to be introduced in solid form such as suspensions of finely powdered material (slurries), in order to avoid lengthy extraction procedures and the use of strong acids, the method must be modified so that it can handle solid, often refractory material.

Due to large size of the particles ($\geq$ 10 μm), two problems are encountered: poor sample introduction efficiency in the conventional, concentric nebulizer; and poor vaporization efficiency at the argon plasma. The nebulizer tends to clog and a large fraction of particles is lost in the spray chamber due to their weight. The conventional argon plasma is not energetic enough to vaporize the analyte.

In this project, a clog free Babington nebulizer was used. A surfactant/thickening agent, polyethylene oxide (PEO), was added to alter such physical properties of the slurry as surface tension, viscosity, and aerosol droplet size. Mixed gas plasma containing small amounts of nitrogen were used. Results showed that, by adding about 5

ppm of PEO, the emission intensity of an analyte increased significantly. Further experiments demonstrated that the signal enhancement resulted from an increase in the nebulizer efficiency brought about by a slight increase in viscosity of the slurry.

The use of mixed gas plasma (Ar + 4% N_2) further improved the emission intensity. Temperature diagnostic measurements of such plasmas indicated that rotational and excitation temperatures are higher than those in a pure argon plasma. The improved temperature is believed to result from the higher thermal conductivity of molecular gases. Nitrogen added to the cooling gas works better than when added to the injector gas. Hydrogen does not seem to work as well as nitrogen, probably because its thermal conductivity is 14 times less than nitrogen. Further studies of the excitation temperature using Fe as the thermometric species, have been helpful in elucidating the mechanism of slurry vaporization in the plasma. There is evidence in this study that mass-transfer rather than heat-transfer is the limiting factor.

With these improvements in the sample introduction and atomization cell, slurries having particle diameters up to 7 μm have been successfully analyzed. This value is 3 times larger than particles injected into pure Ar-plasma without a surfactant. The percent recovery of Ca, Fe, Mg and Pb, are comparable to that obtained from the same samples analyzed as solutions following acid digestion.

DEDICATION

This dissertation is dedicated to:

My parents, brothers and sisters

and to

Hawa, Beresha and Yusuph

ACKNOWLEDGMENT

The successful completion of such an important task like this one required a number of individuals playing part in one way or another. First, I must thank my parents Mr. and Mrs Jusuph Mavura, my brothers and sisters back home in Tanzania, for giving me the necessary support and encouragement. They are the ones who got me started in this long journey. I am indebted to you all because I received more than my share of education in the entire family. Second, I am grateful to my wife Hawa, whose love and friendship have been a constant source of happiness. The entire graduate school experience would not have been possible without her backing. She had to take care of our daughter Beresha (4 years old) and son Yusuph (3 months old), while I spent many hours in the laboratory. The children missed me most of the time in those critical months and years of their development. I am indebted to them.

This research would have never been accomplished without the professional guidance of my advisor Dr. Gary Long. He enriched my love and enthusiasm of *Spectroscopy*. I wish to thank the members of my graduate committee, Dr. Mark Anderson, Dr. Larry Taylor, Dr. John Dillard and Dr. George Sanzone for their time I spent consulting.

Special thanks go to *plaspholks*, Shannon Burcham Schick, Edwin Lancaster, Dr. Gerald Ducatte and Dr. Keith McCleary for the academic and non-academic discussions we shared together. Keith made it possible for us to get a donation of the ICP instrument from Perkin Elmer. This was a timely donation since the other one we had, had seen better days. In this connection I would like to thank Jim Coulter of the electronic shop at Virginia Tech, for his help in putting together the ICP and always being willing to offer his expertise in radio-frequency technology when I needed it.

The glass shop personnel, Andy Mollick and Frans Van Damme, thanks for your expertise in making ICP torches. You were patient with me even when I had to come back to you twice or more per day to repair my burnt quartz torches.

Finally I wish to thank the financial and material supporters of this work: The US EPA, Virginia Water Resources Research Center, DuPont Chemicals and the Graduate Student Assembly of Virginia Tech.

TABLE OF CONTENTS

LIST OF FIGURES

LIST OF TABLES

Chapter 1

INTRODUCTION

Successful analytical atomic spectrometry experiments require the optimization of two fundamental areas: the efficiency of sample introduction into the instrument and the analyte atomization. The sensitivity of any particular method of analysis depends on these two efficiencies. For aqueous samples, the liquid is readily introduced into the atomization cell using concentric, pneumatic nebulization techniques. Measurements can be made using a combustion, electrothermal, or plasma environment. The atomization cell is either atomic absorption or atomic emission. Although atomic absorption spectrometry techniques (Flame Atomic Absorption and Graphite Furnace Atomic Absorption) have enjoyed enormous popularity in the last three decades, inductively coupled plasma atomic emission spectrometry (ICP-AES) has been widely utilized in the last decade for many analyses involving environmental samples. The ease of sample introduction for liquids, coupled with the excellent limits of detection of this spectrometric method, provide the analyst with the ability to perform rapid multi-element determination of the metals in aqueous environmental samples. However many environmental samples are not aqueous in nature, but are solid, such as soils and sediments. These solid samples must be transformed to an aqueous matrix for analysis using conventional nebulization technique.

An alternative to solution introduction into ICP-AES is slurry injection, whereby the sample in powder form, typically < 10 μm particle diameter is suspended in water and directly introduced into the plasma. Due to the solid nature of the slurry sample, a special type of nebulizer which does not clog during the operation must be utilized. The

pure argon plasma which is suitable for a sample in solution matrix, has to be modified since it is not sufficiently energetic for slurry sample atomization.

The purpose of this dissertation is to develop a method for the determination of metals in slurry matrices using the ICP-AES technique. It is apparent at this point that there are two major problems in slurry analyses: poor formation and transport efficiency of aerosol from the nebulizer to the plasma also poor atomization and excitation efficiency at the conventional argon plasma. To understand the magnitude of the problems and the design of the "new" technique, it is appropriate to first review several relevant topics including: the ICP emission spectrometry apparatus, characteristics of the ICP, mixed gas plasmas, slurry nebulization, the Babington nebulizer, and the role of surfactants in the formation and transport of aerosols.

Typical ICP Emission Spectrometry Apparatus: The apparatus presented in Figure 1, consists of a nebulizer, usually concentric or cross flow or a variety of these, a spray chamber, and a torch. The sample is drawn into the nebulizer capillary by a controlled flow of argon through the outer jacket. Flow rates are typically 0.8 L/min argon and 1.0 L/min analyte liquid. The aerosol formed by the nebulizer is passed into a double spray chamber, where the larger droplets collect in the drain. About 2% of the original sample passes into the center tube of the torch and into the ICP discharge.

Characteristics of the ICP: The inductively coupled plasma is a partially ionized gas, typically argon, which is less than 1% ionized in the plasma. An ICP discharge is caused by the ionizing effect of a radio frequency field on a flowing gas. Argon gas flows upward through a quartz tube, around which is wrapped a copper coil or solenoid. The coil is energized by a radio frequency generator operating at 5 to 75 MHz

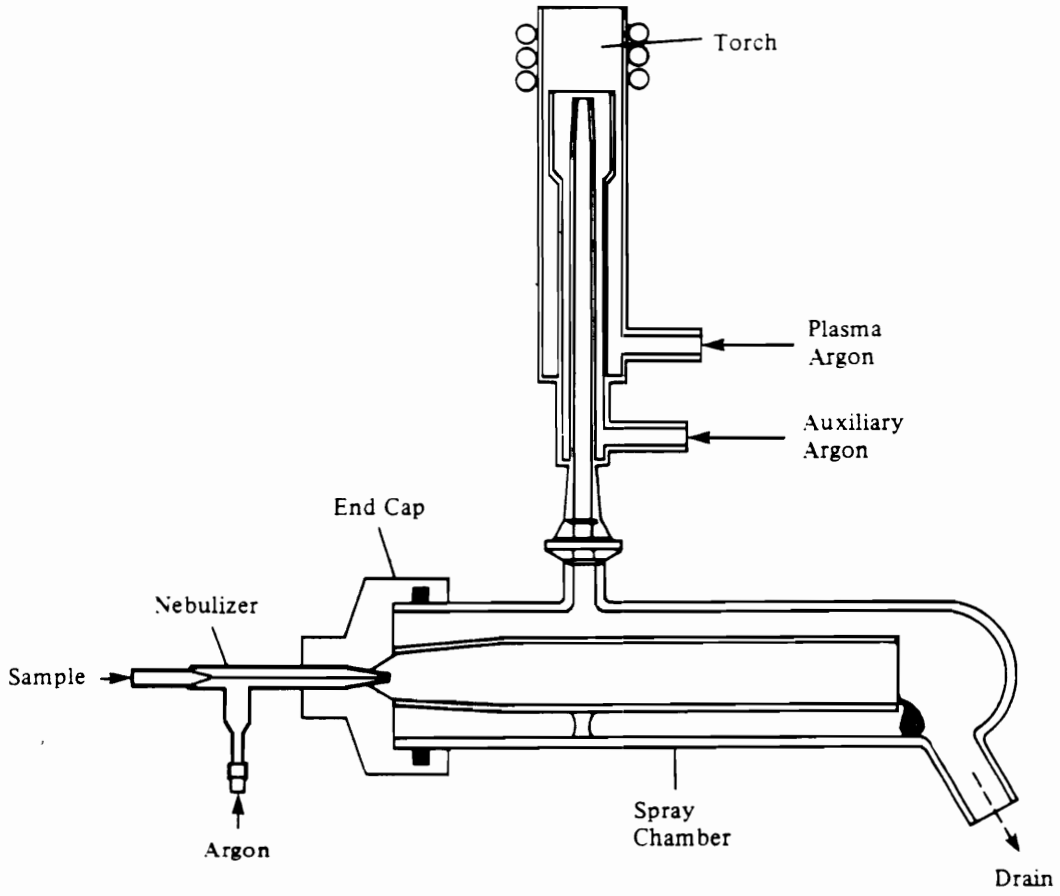

Figure 1. Typical nebulizer, spray chamber, and torch for Inductively Coupled Plasma emission spectrometry.

(From reference 1)

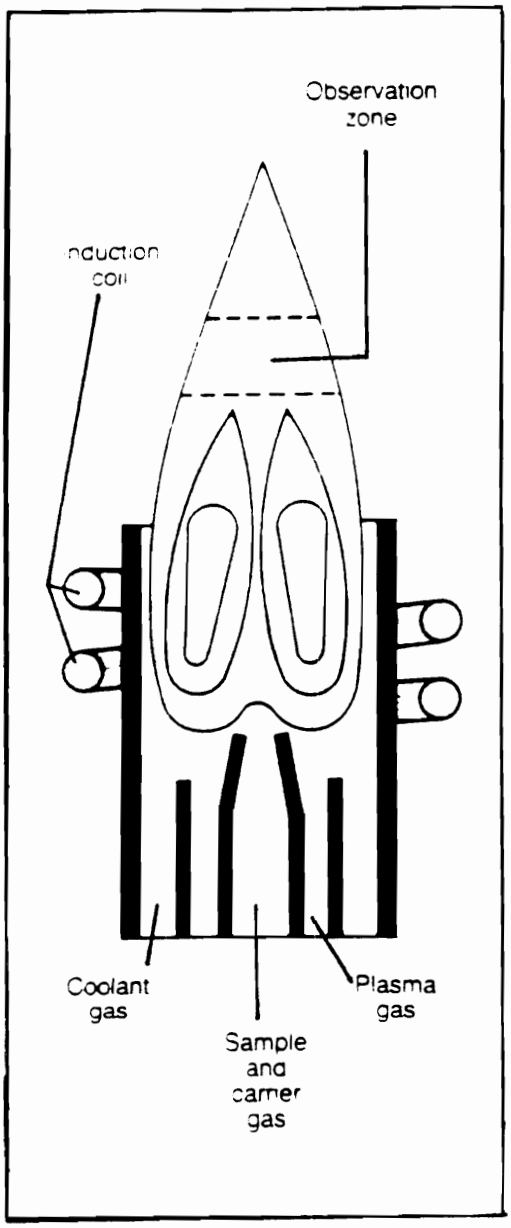

Figure 2. Diagram of an argon plasma.
(From reference 2)

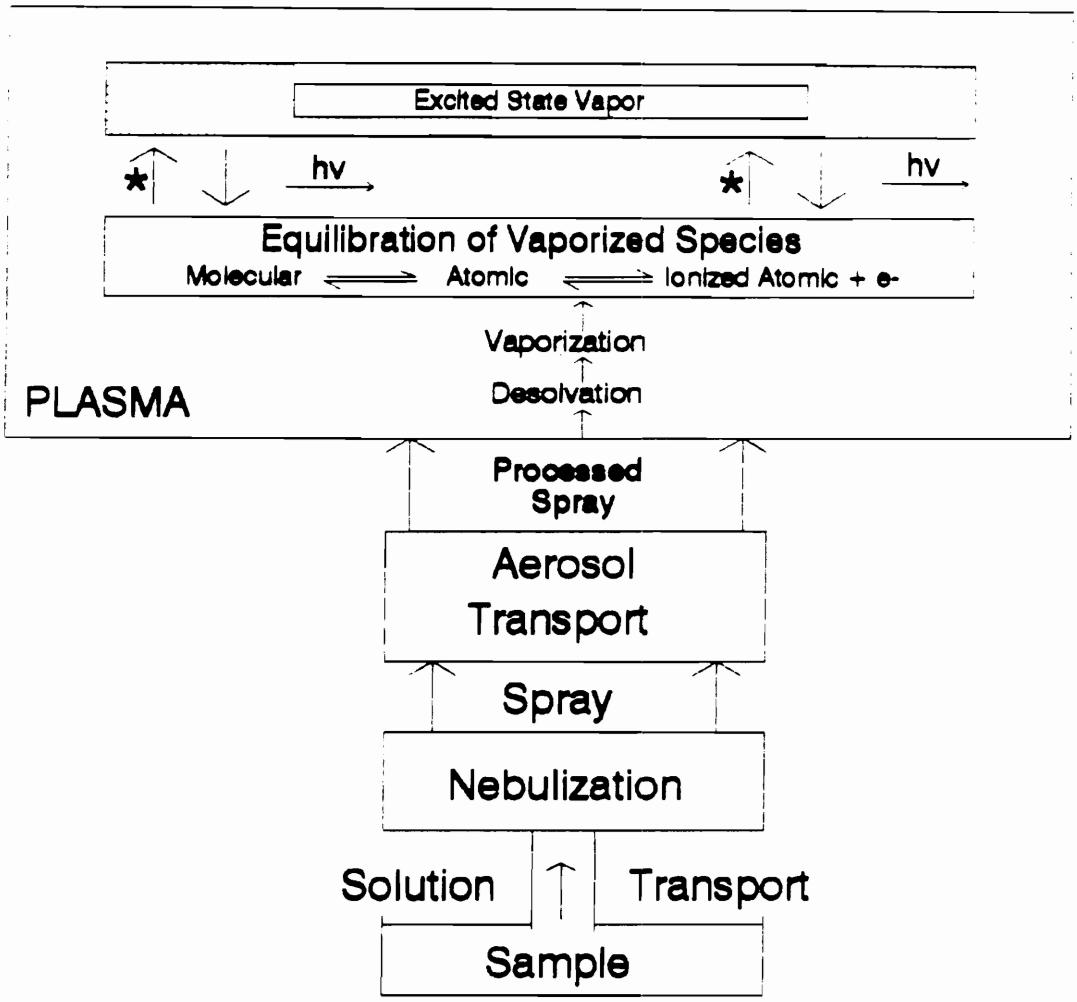

Figure 3. Block diagram for sample transport/excitation processes. (From Reference 1)

Ar-N_2 ICP is the most common, Ar-H_2 [5, 6], Ar-Air, Ar-O_2 [7 - 9] and Ar-He [10, 11] have been used in the outer flow to generate mixed gas plasmas for ICP-AES and ICP-MS. When Ar is replaced with other gases, the physical characteristics of the plasma are altered. Compared to the Ar ICP, mixed gas plasmas are physically smaller, leading to generally lower observation heights in the plasma [12]. The reduction in volume has been interpreted in terms of the energy needed for the dissociation of the diatomic molecules. As a result of the energy expended for the dissociation process, reduced temperature and diminished electron number density are expected in the outer region of the discharge, and therefore the shrinkage. This phenomenon, called thermal pinch, has also been explained in terms of gas transport properties such as thermal conductivity and specific heat [13]. In contrast to Ar, the thermal conductivity and specific heat capacity of nitrogen do not increase monotonically with temperature, but rather, they reach a maximum at 6000 K, fall to a minimum at about 8000 K, and then rise with increasing temperature. This plot is demonstrated in Figure 4 [14]. Thus, the temperature of an Ar-N_2 ICP may pass through an inflection point where the discharge appears smaller [13].

It has also been observed that if a molecular gas is used to support the discharge *i.e.* as the outer gas, the diameter of the axial channel usually becomes smaller than that of an Ar ICP. The shrinkage enhances sample-plasma interaction and consequently the emission signal of analyte. This is due to increased energy density of the plasma in the central/axial channel. On the other hand, for Ar supported ICP, *i.e.* pure argon as the outer gas, the diameter of the axial channel increases and the plasma length diminishes as the composition of the injector gas is changed from pure Ar to pure molecular gas. Since the outer diameter of the plasma toroid remains unchanged [15], the thickness of the toroid is reduced. It is assumed that a portion of energy in the vicinity of the axial channel is used to dissociate the diatomic injector gas, thus reducing the temperature of

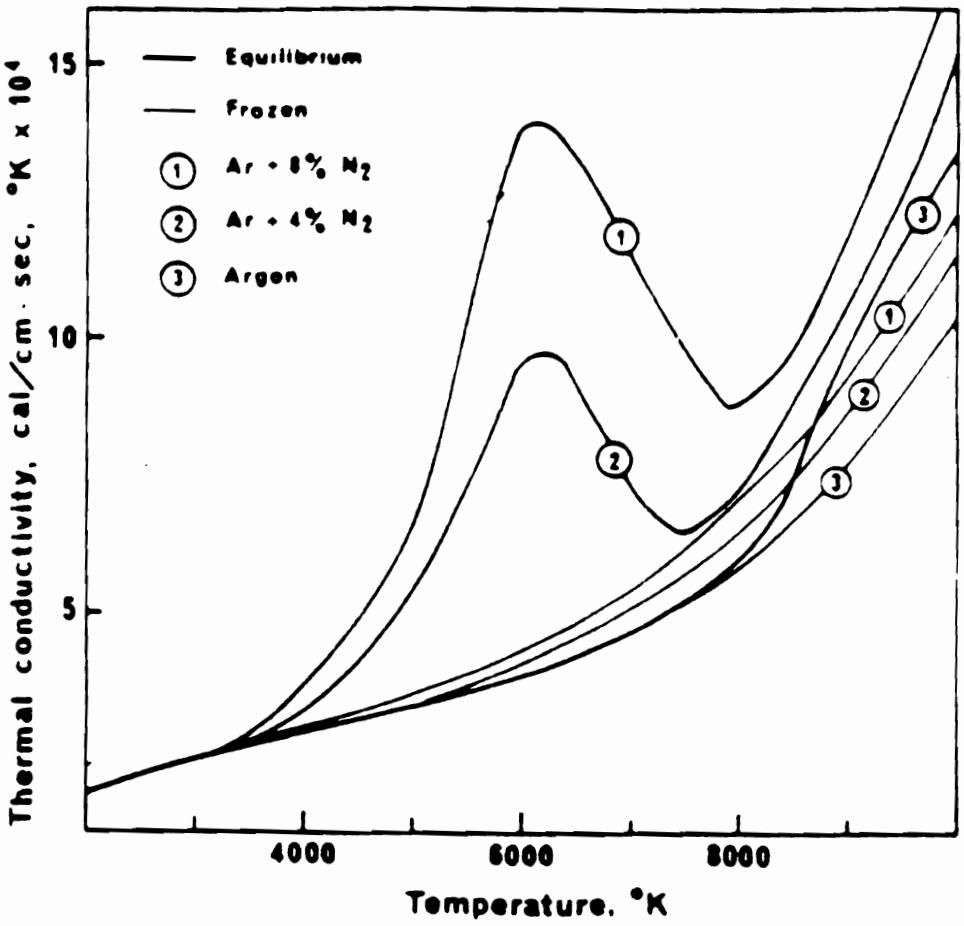

Figure 4. Effect of molecular gas (nitrogen) on plasma. At equilibrium the enhanced thermal conductivity increases the plasma temperature. For non-equilibrium (frozen), the effect is not apparent.
(From reference 14)

the axial channel [13]. This overall reduction of plasma size and in particular the toroid thickness, results in reduced sample-plasma interaction evidenced by a reduced analyte emission signal [15 - 17].

Experimental and theoretical studies have documented that Al_2O_3 or CaO particles decompose faster in plasma sustained in Ar-N_2 or Ar-H_2 than in pure argon plasma [12, 14]. For this reason mixed gas ICPs generally are more suitable than Ar ICP for direct elemental analysis of airborne particulates, slurries and solids.

Studies on Analytical Plasma Diagnostics: In addition to characterizing different types of plasmas, including pure argon and mixed gas plasmas in terms of emission capabilities, it is necessary to characterize them quantitatively in terms of temperature. Temperature is one of the most important criteria used to assess the properties of analytical ICPs. This property can provide insight on the various reaction mechanisms prevailing in the plasmas, the extent of departure from local thermodynamic equilibrium, and most important, the role of different gaseous species in exciting the analyte.

A study of the literature on temperature values reported for mixed gas, either cooling or injector, reveals a great variation. For example, rotational temperatures reported by Montaser [12], range from 2300 to 8900 K depending on the rf power used, the frequency, observation height, type and amount of the modifier gas. Similarly, excitation temperatures have been measured using a number of different variables. Kornblum and Galan [18] have reported a range from 2000 to 12000 K depending on plasma conditions, observation height and the actual temperature measurements.

It would be extremely difficult to compare these temperatures in such widely differing plasma conditions and especially where modifier gases are introduced either as

coolant or injector. The difference in temperature values can only be meaningful if the same temperature measurement conditions are used, including same species, same spectral lines, same transition probabilities, same power, frequency, type and amount of gas introduced. The relative effect of molecular gases and the influence of the technique by which these gases are introduced will be more apparent under these fixed experimental conditions.

This research provides comparative results for the two modes of introducing mixed gas (*i.e.* as injector and as cooling gas) into ICP. It also compares the effect of nitrogen and hydrogen, the two common molecular gases used. For this comparison, rotational and excitation temperatures have been measured as increasing amounts of nitrogen and hydrogen are separately introduced. Thus, temperature data have been obtained for (a) Ar-N_2 coolant, (b) Ar-N_2 injector, (c) Ar-H_2 coolant (d) Ar-H_2 injector. The intensity of Fe atomic emission spectra were used to calculate the excitation temperature whereas molecular bands of N_2^+ and OH were employed to determine the rotational temperature of the plasma. Two sources of Fe were used in T_{exc} diagnostics; namely aqueous solution (Fe^{2+}) and Fe_2O_3 slurry.

Slurry Nebulization: Slurry injection is especially required for elemental analysis of refractory material which can only be dissolved by a treatment with high boiling point acids. Such compounds include ceramic powders, *e.g.* Al_2O_3, SiC, Si_3N_4, and ZrO_2 and many geological samples, river sediments and estuarine sediments [19, 20]. After the sample has been prepared by grinding (< 10 μm) and made into a suspension with aqueous medium (normally 1% m/v), it is introduced into the plasma via a nebulizer and spray chamber. Simple aqueous solutions are used to calibrate the method. For this direct calibration with aqueous solutions to be performed, two criteria must be satisfied if

accurate analyses are to be obtained. These criteria are: (a) that both the analyte transport efficiency of the slurry particle, and (b) the subsequent atomization efficiency of that particle must be identical to that of a simple aqueous solution [21]. If either or both of these conditions are not met then the analytical accuracy of slurry nebulization ICP-AES is degraded.

The two efficiencies are relatively poor due to the very nature of analytes in slurry samples, often large, heavy and refractive particles. In the previous section it was discussed how the atomization efficiency could be enhanced by the use of mixed gas plasma. Slurry analyte transport could be improved by (1) the use of a proper nebulizer and a spray chamber and (2) modification of the slurry with surfactants or thickening agents. The following sections will discuss the fundamental characteristics of each of these areas.

The Nebulizer: A nebulizer is a device which produces the sample aerosol that is required for atomic spectrometric analysis. The standard ICP nebulizer for introducing aqueous samples is the concentric type, in which support gas (normally argon) is passed through a narrow glass tube. The reduced pressure causes the liquid sample to be drawn up a small tube concentric with or at right angles to the gas tube [22] Although some ultrasonic nebulizers and fritted disk systems are capable of introducing excess of 90% of the analyte solution into the plasma, concentric nebulizers have achieved widespread popularity because they are less expensive, simpler, and still yield acceptable detection limits for many applications [23, 24].

Although this type of nebulizer is excellent for solutions, being capable of 5 -10% efficiency in production of analytically useful droplets, its utility for slurries is rather

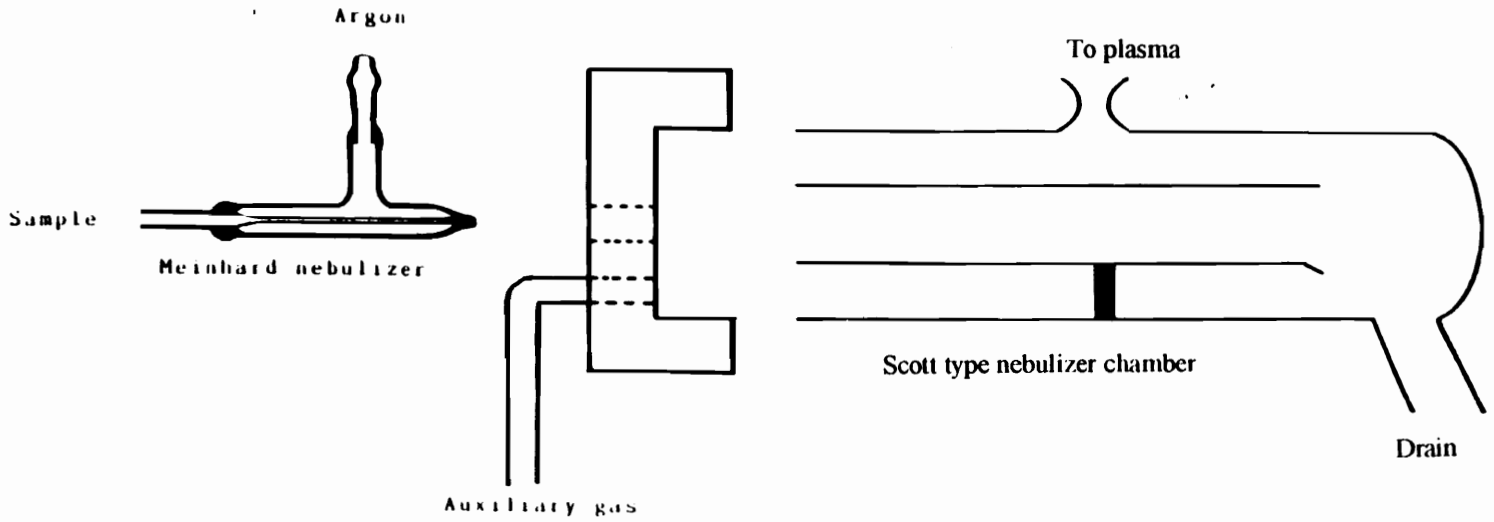

Figure 5. Schematic of a Meinhard (concentric) nebulizer and a Scott type spray chamber.

limited. As Figure 5 shows, the sample must pass through a relatively small capillary tube. Slurries tend to clog this orifice. To avoid this problem, Robert S. Babington devised a non-clogging nebulizer [25]. In this type of nebulizer, shown in Figure 6, the sample is pumped over a hollow bulb which has a tiny orifice on the side. The nebulizing gas is passed through this orifice under pressure, which creates an aerosol by impact of the gas stream with the flowing liquid. The major advantage of this type of nebulization is that, since the sample does not pass through the orifice, clogging of the nebulizer is eliminated.

The Spray Chamber: A spray chamber is placed between the nebulizer and plasma. It functions as a droplet separator and a flow buffer to remove large droplets and thereby improve the stability of analytical signals [26]. The removal of large droplets is inevitably accompanied by a reduction in the transport efficiency of aerosol and analyte to the atomization/excitation source. Measurements carried out on a typical ICP nebulizer/spray chamber system reveal that more than 98% of the aerosol is lost to waste [27]. As a result, the transport efficiency of a typical ICP system is only in the range of 0.5-2%. In addition to this, fine droplets are suspended and circulate inside the spray chamber, resulting in relatively long memory effect due to long wash-out times.

Hieftje and associates [26] have reported that a double-pass Scott-type spray chamber (Figure 5) with a volume of about 200 mL typically used in ICP is better than a smaller, single-pass horn-like shaped chamber in several aspects. Compared with the Scott-type, the smaller one (about 50 mL) has at least 30% higher sample utilization efficiency, 2-3 times shorter sample clean-out time, half the cost, and simplified construction. Moreover, the authors report that it offers better signal-to-background ratios, detection limits and precision.

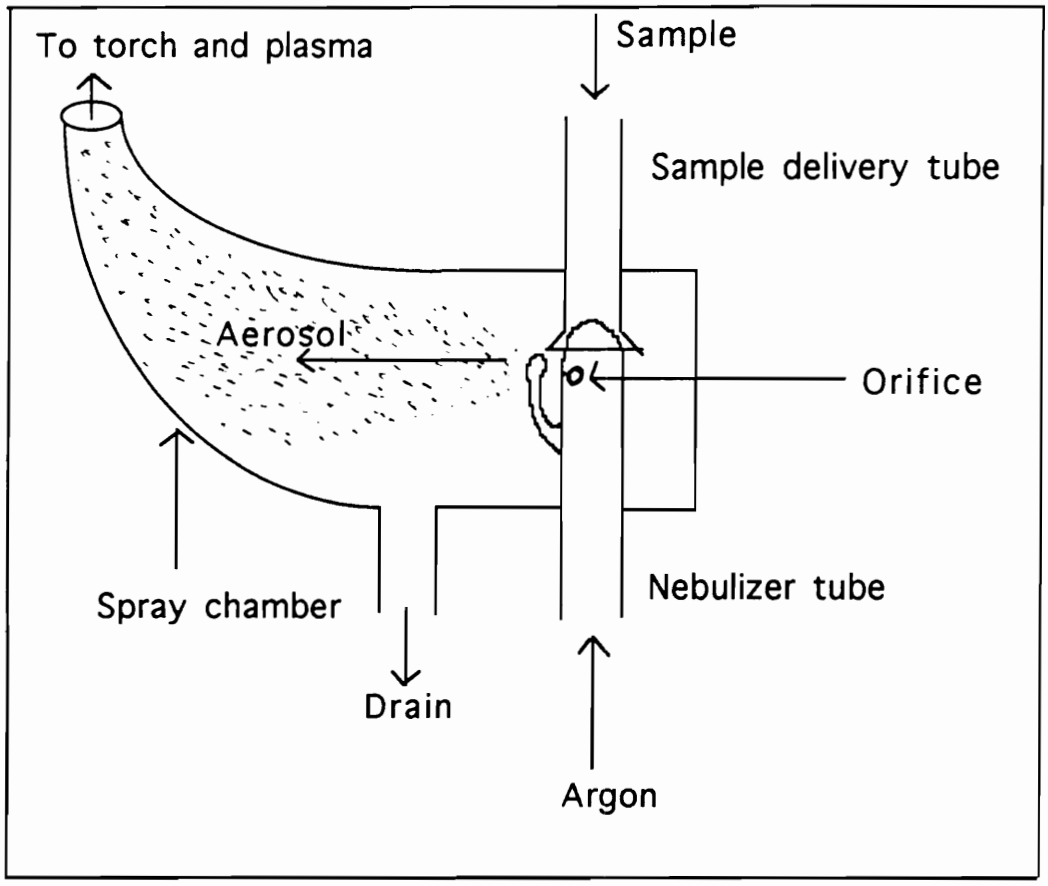

Figure 6. Babington-type nebulizer and horn-shaped spray chamber.

For these reasons in this study, the Babington nebulizer was used with a smaller, horn shaped spray chamber (Figure 6) to introduce slurry aerosol into the ICP.

The Role of Surfactants: Physical properties of a solution such as surface tension and viscosity influence the characteristics of the primary aerosol. It has been suggested by some workers that the addition of surfactants to the aqueous solutions lowers the surface tension and hence improves transport efficiency as a result of producing an aerosol which contains smaller, more easily transportable droplets [28 - 30]. Currently, there is a controversy over whether surfactants actually improve the signal in atomic spectrometry. Some workers report significant improvement in analyte signals [31 - 34], whereas others have find little or no effect [35, 36]. It has also been reported that anionic surfactants such as sodium dodecyl sulfate (SDS) tend to improve the sensitivity of cationic analytes, whereas cationic surfactants such as hexadecyltrimethylammonium bromide, CTAB, give rise to improved signal from anionic analytes. On the other hand, non-ionic surfactants such as Triton X-100 have no effect on either ionic or anionic analytes [37].

It should be pointed out that the above mentioned surfactant studies were conducted using analytes in solution and flame atomic absorption spectrometry (FAAS) with pneumatic nebulizers. There are no reports in the literature on the influence of surfactants on the emission signal for slurry injection technique in ICP-AES. This technique as discussed above possesses great potential for analysis of ceramics, geological and other refractory samples. Since the transport and atomization efficiency of such samples is particularly poor, the addition of a surfactant may enhance this process.

Polyethylene oxide (PEO), a high molecular weight polymer is a water soluble non-ionic surfactant which can increase the viscosity and reduce surface tension of aqueous solutions and slurries [38]. The influence of this surfactant on the emission

intensity of slurries is studied as well as on changes in physical properties of the slurries, including surface tension and viscosity. The changes in droplet sizes formed as a result of changes in these physical properties are investigated to aid in the interpretation of the emission pattern.

Organization of the Dissertation: This dissertation is organized according to the following chapters. Chapter two is a description of the experimental equipment, materials and chemicals used in this entire study. Also, in this chapter is a description of major techniques such as surface tension and viscosity determination. Chapter three is a presentation and discussion of the effects of both the surfactant, PEO, and mixed gas plasma (Ar/N_2) on the emission signal of an element in a slurry matrix. Chapter four deals with measurements of plasma temperatures. Rotational and excitation temperatures of mixed gas plasma are presented for both hydrogen and nitrogen. This is a comparative study of the influence of introducing N_2 and H_2 in the plasma either as part of the cooling gas or injector gas. Data from these measurements are also used to elucidate the mechanism of analyte vaporization in the plasma. Chapter five evaluates the application of the optimized method, that is, modified sample injection technique and mixed gas plasma as per previous chapters for analysis of real samples. These samples are standard reference materials from the US EPA. The emphasis here is to study the percent recoveries of metals and compare these results with those obtained from the conventional method (acid digestion) prior to analysis with ICP. The final chapter summarizes the results of the previous chapters and presents some the conclusions.

The work presented in this dissertation is an investigation of sample injection into the ICP as slurry instead of solution. Two fundamental aspects are examined. (1) The possibility of enhancing sample introduction with the aid of a surfactant together with the

use of a Babington-type nebulizer and (2) the possibility of enhancing the atomization/excitation capability of the plasma by properly modifying it with molecular gases.

Chapter 2

EXPERIMENTAL CONDITIONS

Reagents: Aluminum oxide was purchased from Fisher Scientific (Fair Lawn, NJ). Polyethylene oxide, iron (III) oxide and aluminum metal were purchased from Aldrich Chemical Company (Milwaukee, WI). Plasma gases including argon, nitrogen and hydrogen were purchased from Airco, (Murray Hill, NJ) and were of analytical grade. Stock solutions of 1000 ppm of aluminum were prepared by dissolving 1.000 g of high purity aluminum metal wire in 50 ml of hot hydrochloric acid. The resulting solution was diluted to 1.000 L with distilled/deionized water. Calibration solutions were made by diluting appropriate volumes of the stock as needed. All chemicals were reagent grade and were dissolved in distilled deionized water.

Instrumentation: The instruments used in this study are summarized in Table 1 and a schematic presentation of the instruments is shown in Figure 7. The plasma spectrometer was a Perkin Elmer ICP/6000. A radio-frequency power supply was used to supply up to 2.5 kW of rf power at a frequency of 27.12 MHz. The torch was housed in a torch box which is a shielded rf enclosure. In operation, argon gas flows through the torch, and a plasma was generated inductively by applying about 1.25 kW of rf energy from a copper coil around the torch. To avoid overheating, a continuous, 0.5 L/minute water flow through the rf was required. The sample to be analyzed was introduced via a plastic capillary tube at the front of the torch unit, through the center tube, into the plasma zone.

Table 1. Instrumentation

Component	Model / Size	Manufacturer
ICP Generator	ICP / 6000, 27.12 kHz	Perkin Elmer Norwalk, CT
Monochromator	Model 5000, Czerny-Turner 0.41 m focal length	Perkin Elmer
Data station	7500 Professional Computer	Perkin Elmer
Printer	PR-210	Perkin Elmer
Data acquisition software	Series 7000 Idris System	Perkin Elmer
Nebulizer	Babington	Precision Glassblowing, CO
Spray Chamber	single-pass, conical/horn-like	Laboratory built
Torch	Demountable, 3 mm i.d. tip	Perkin Elmer
Peristaltic Pump	CSA-Minipuls 2	Perkin Elmer
Magnetic Stirrer	PC-351	Corning
Grinder	Attrition Mill grinder, Model 1058	Teledyne Engineering Marion, MA
Particle Size Analyzer	Elzone Monitor	Particle Data, Inc. Elmhurst, IL
Viscometer	Ostwald	Fisher Scientific, Pittsburgh, PA
Dynamic Contact Angle Analyzer	DCA-322	Kahn Instruments, Carritos, CA
Sonicator	Branson, B-22-4	Smith Cline Co., Conn. USA

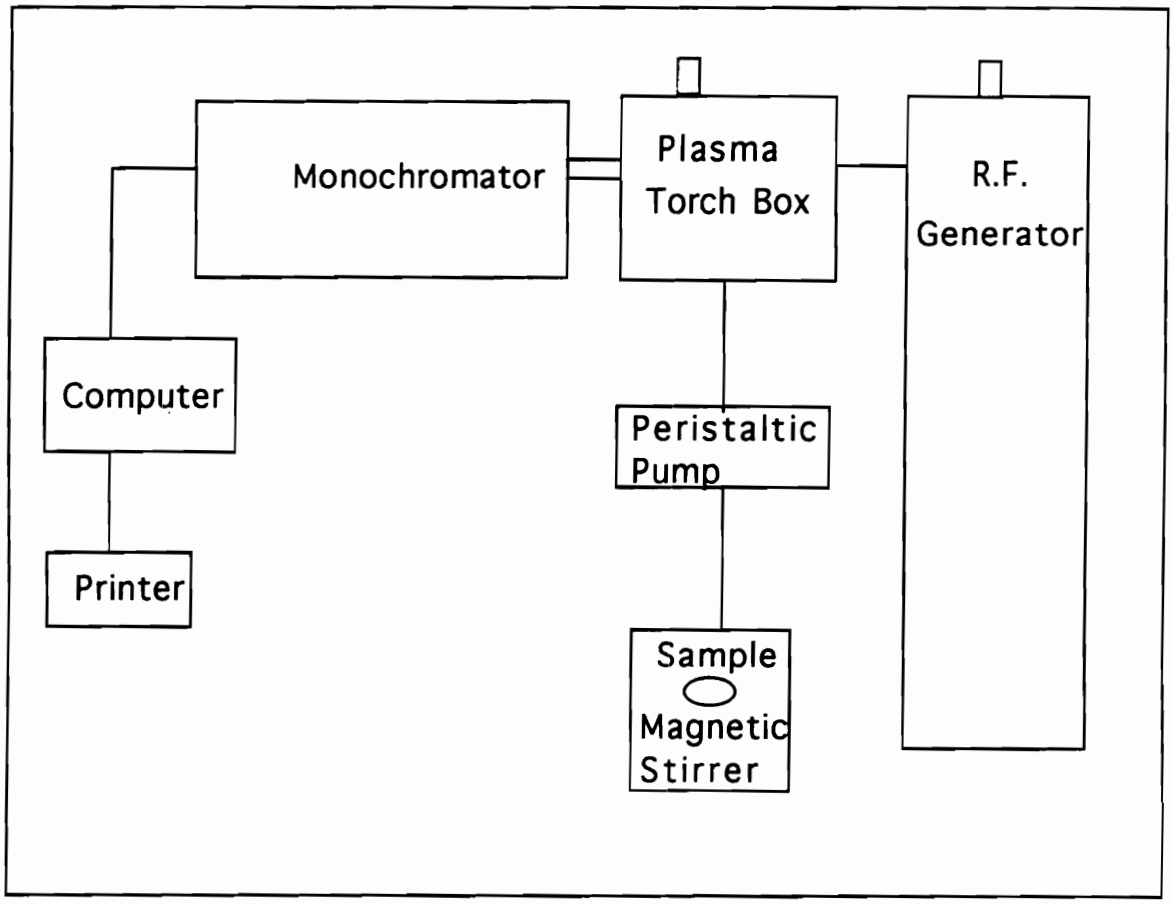

Figure 7. Schematic of apparatus for slurry injection into ICP.

The plasma emission signal was focused onto the slits of the monochromator via the transfer optics. A height adjustment enabled different vertical zones of the plasma to be viewed, to obtain the best signal-to-background ratio. The monochromator was a Czerny-Turner type, 0.41 mm focal length. The resolution was 0.05 nm/mm and nominal bandpass was 0.02 nm. The data station (Model 7500 Professional Computer) was the controller of the ICP/6000. Some of the inherent features of the computer are: a 16-bit Motorola MC 68000 microprocessor, 640K Random Access Memory (RAM), a 10-Megabyte hard drive disk, and two double-sided double-density floppy disk drives [39].

It was mentioned in the previous chapter that a Babington nebulizer was necessarily used for introducing samples to the plasma. Characteristics of the Babington nebulizer together with data used in the calculation of droplet size are presented in Table 2. Also presented in this table are the optimized operating conditions of most of the experiments. When N_2 or H_2 was introduced into the Ar cooling gas stream or injector gas to produce the mixed gas plasma, an equivalent amount of Ar was reduced from the main stream so as to maintain 15 L/min total gas flow. Nitrogen was introduced through a 150-mm rotameter.

Slurry Preparation: Samples were prepared by grinding chromatographic grade powdered alumina of diameters ranging from 80 to 200 mesh (177 to 74 μm) using dry grinding techniques. In this method, 3 mm stainless steel beads were mixed with the powdered sample in a closed container of the grinder. This device was an attrition mill, which grinds the sample by friction. Inside the container there is a vertical shaft with horizontal stirrers. The shaft was connected to an electrical mortar and can be rotated at variable speeds. In this work, a speed of 2500 rpm was chosen. Achieving a particle mean diameter of 4 μm required 30 minutes of grinding. In all the experiments, unless

Table 2. Operating conditions

Forward power	1.25 kW
Reflected power- Ar plasma	10 W
Reflected power- Ar + N_2 plasma	25 W
Cooling gas flow rate	15 L/min
Auxiliary gas flow rate	0.4 L/min
Nebulizer gas flow rate	3.0 L/min
Diameter of aerosol gas nozzle	0.2 mm
Diameter of sample injector	2.0 mm
Aerosol gas flow rate	0.8 L/min
Sample feed rate	1.0 mL/min
Gas velocity	2.5×10^{4} m/s
Sample velocity	5×10^{-2} m/s
Surface tension of water (26°C)	70 dynes/cm
Viscosity of water (26°C)	0.0089 dynes s/cm^2

otherwise stated, a 0.5% (w/v) suspension was made as follows: 0.5 g of aluminum oxide was mixed with the appropriate amount of PEO, then distilled/deionized water was added to make 100 mL. Polyethylene oxide concentrations of 5.0 mg or higher, required about 30 minutes to dissolve completely. Iron (III) oxide used in excitation temperature determination, did not require extra grinding, since the mean particle size of the purchased sample was < 5 μm.

Standard Reference Materials (SRM) from the US Environmental Protection Agency (EPA), Research Triangle Park, NC were selected on the basis of their particle size. No attempt was made to grind the samples due to their small quantities, about 1 or 2 grams each. The dry grinding method utilized in this study required a relatively large amount, about 10 grams, since a large fraction is necessarily lost on the surface of the grinding steel balls. Table 3 lists the SRMs that were analyzed, and they include those with large (≥ 10 μm) and small (≤7 μm) mean diameter.

Sample Introduction: During introduction of the slurry into the instrument, the suspension was continuously stirred using a magnetic stirring bar in order to maintain a homogeneous mixture. However when iron (III) oxide was analyzed, an ultrasonic bath was used to homogenize slurries, instead of a magnetic stirrer (which would attract the oxide from the sample). A peristaltic pump was used to introduce slurries into the plasma through the nebulizer. The Babington nebulizer shown in Fig. 5 is a variant of the cross-flow nebulizer [12]. It consists of a glass delivery tube and nebulizer tube. The nebulizer tube has a small horizontal gas orifice and an impaction bead. The sample is introduced down the delivery tube and forms a thin film over the outside surface of the nebulizer tube. Primary aerosol droplets are formed at the orifice as a result of gas

Table 3. List of Standard Reference Materials analyzed

Sample ID	Nature
NIST - 1575	Pine needles
BCR - 146	Sewage sludge of mainly industrial origin
BCSS - 1	Marine sediment
BCR - 176	City waste incineration ash
NIST - 1579	Powdered Lead base paint

NIST - National Institute of Standards and Technology

BCR - Community Bureau of Reference

BCSS - a Canadian Standard Reference Authority

rupturing the film of liquid. Secondary droplets are formed at the impaction bead. The sample is introduced into the plasma through the inner tube of the torch.

Viscosity Measurements: The viscosity of slurries was measured using an Ostwald viscometer as explained in Daniels *et al.* [40]. This method is based on measuring relative viscosities by comparing the flow rate of the various slurries. The time for the liquid to fall from an upper mark in the capillary tube to the bottom mark was determined. The measurement was repeated until four consecutive measurements were within 0.5 second. Then the following equation was used to calculate the viscosity:

$$\eta_1 = \frac{\rho_1}{\rho_0} \times \frac{t_1}{t_0} \eta_0 \qquad (1)$$

where ρ_1 and ρ_0 = densities of the slurry and pure water respectively
t_1 and t_0 = relative times of flow for slurry and water
η_1 and η_0 = relative coefficients of viscosity for slurry and water.

Since the density of slurries was measured in g/cm^3 and time in seconds, viscosity is reported in dyne seconds per cm^2. Where 1 dyne s/cm^2 equals 1 g/cm/s or 1 poise [40].

Surface Tension Measurements: The surface tension was determined by using a Dynamic Contact Angle Analyzer, DCA-322 [41]. Since the method requires the use of a clean glass slide and clean liquid, the surface tension of aqueous solutions of polyethylene oxide in deionized/distilled water were determined instead of slurries. The surface tension of solutions and slurries is not likely to be different because surface tension is a function of the concentration of the dissolvable substances, not of dispersed particles [19, 32]. The equation that the instrument used for calculation of surface tension was:

$$F = \frac{\gamma \times P \times \cos\theta}{0.981} \qquad (2)$$

where F = Sample force at zero immersion depth as determined by the balance (mg)

P = Perimeter of sample (slide) at interface (cm)

γ = Surface tension (dynes / cm)

cos θ = Cosine of contact angle. The angle is assumed to be zero and cos 0 = 1

0.981 = Conversion factor, mg to dynes.

Plasma Temperature Measurements: Plasma temperatures reveal how the energies of the plasma species shift among rotational, vibrational and electronic levels. The excitation temperature of a plasma is a measure of the population distribution of energy levels in the plasma discharge. The knowledge of this distribution gives an indication of the excitation capabilities of the plasma. As most molecules are in the excited rotational levels at ordinary temperature, T_{rot} is considered to be a good approximation to the gas kinetic temperature, T_{kin} [42]. Excitation and rotational temperatures were measured for plasmas with different amounts of molecular gases. In both cases suitable thermometric species (probes) were selected. For rotational temperature, the probes were the hydroxyl radical (OH) and nitrogen monopositive ion (N_2^+). The former was monitored when water was aspirated and in the presence of hydrogen, *i.e.* mixed gas plasma, whereas the latter was monitored as nitrogen was introduced. On the other hand, Fe was used as a probe for excitation temperature

measurements. Two sources of Fe atoms were utilized; a 1000 ppm aqueous solution of Fe^{2+} and a 0.1% (w/v) Fe(III) oxide slurry. This slurry was equivalent of 1000 ppm Fe.

Data Acquisition and Presentation: The data were collected by using standard ICP/6000 operating procedures. The resolution of the spectrometer was 0.02 nm. The integration time was set at 0.2 second. All spectrometric data are reported here as the arithmetic mean of three replicate samples, from the same preparation, each of which was determined 3 times, that is, three integrations. Other data such as viscosity and surface tension were also measured 3 times. Error bars reflect the standard deviation of each data set.

Chapter 3

EFFECT OF A SURFACTANT AND MIXED GAS PLASMA ON SLURRY INJECTION INTO ICP

Introduction: Changes in physical properties of the slurry including viscosity and surface tension, and their overall effect on the emission intensity of aluminum, as a consequence of the presence of PEO, are being presented and subsequently discussed in this chapter. The relationship between these physical properties and the size of aerosol droplets formed by the nebulizer is demonstrated using the Nukiyama-Tanasawa equation [43]. The effect of sample flow rate onto the nebulizer on emission intensity is determined to characterize the performance of the nebulizer, in the presence and absence of PEO. The molecular weight of PEO used in this study was 4×10^6. The impact of molecular gases (nitrogen and hydrogen) in the plasma on the atomic emission characteristics of aluminum is accessed.

Effect of Polyethylene Oxide: The effect of the concentration of polyethylene oxide in the Al_2O_3 slurry on the emission signal of Al (I) at 396.152 nm is shown in Figure 8. Emission signals were recorded for slurries containing between 0 and 10 mg PEO per 100 mL of slurry (100 ppm). There was a significant enhancement of signal corresponding to a concentration level of 0.5 mg/100 mL PEO. This enhancement was about 50% higher than the signal obtained from slurries containing no PEO. Subsequent additions of PEO caused a reduction of the signal such that a concentration of 10 mg PEO, caused signal reduction to be at almost background levels.

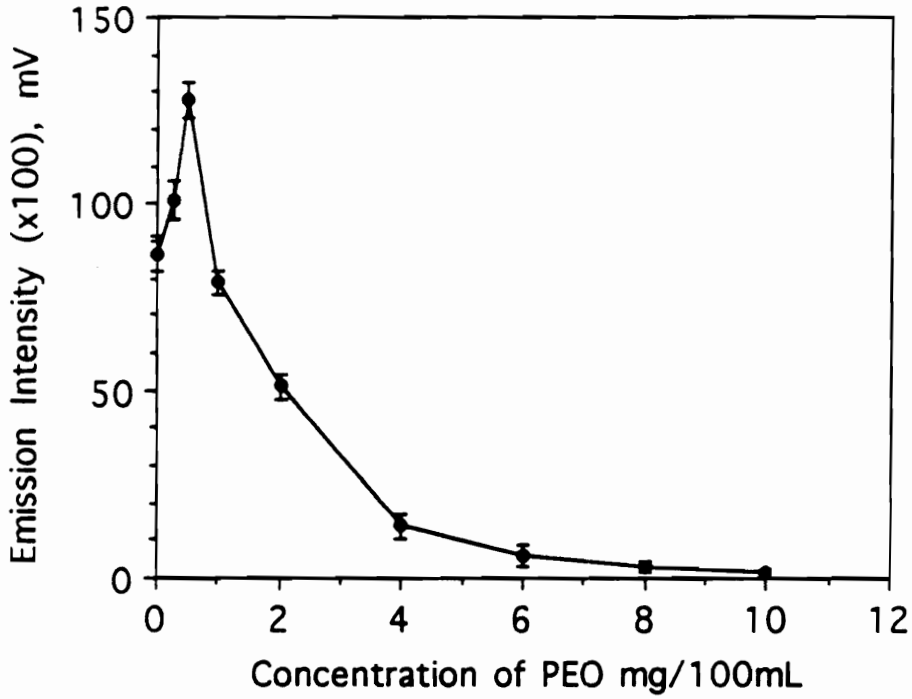

Figure 8. Effect of PEO on alumina slurry emission. Sample: 0.5% (w/v) Al_2O_3 suspension in water. Observation height: 10 mm above coil in a 1.25 kW, Argon-Nitrogen (4%) mixed gas plasma.

Polyethylene oxide has two important effects in aqueous media; decreasing the surface tension and increasing the viscosity as depicted respectively in Figures 9 and 10 and also summarized in Table 4. These illustrations indicate that small amounts of PEO caused significant changes in surface tension as well as viscosity. The surface tension decreases with concentration of PEO up to about 2 mg/100 mL and then assumes a nearly constant value. This concentration value (2 mg) is the critical micelle concentration of this particular PEO (4 million). Beyond this concentration, the surfactant forms aggregates [44].

Surface tension is the property of a liquid evidenced by the apparent presence of a thin elastic membrane along the interface between the liquid and a vapor phase, resulting in a contraction of the interface and reduction of the total interfacial area. Thermodynamically, it is the excess free energy per unit area of interface resulting from imbalance in the cohesive forces acting on liquid molecules at the surface [44]. The reduced surface tension of the aqueous media favors the formation of smaller aerosol droplets because small droplets have larger interfacial surface area [45]. The larger surface area is a result of lower tension, that is, less tension at the surface means larger surface area. The effect of viscosity on droplet size can be explained as follows: formation of a droplet requires that the volume of the droplet be detached from the bulk of the liquid [46]. The greater the viscosity, the more force required to detach the droplet, resulting in larger droplets.

Theoretically, increasing the concentration of PEO has a tendency to: (a) decrease droplet size due to decreasing surface tension, and (b) increase droplet size due to increasing viscosity. The two physical properties are therefore competing in determining the size of droplets. The estimation of droplet sizes was performed by employing the Nukiyama-Tanasawa equation [43]:

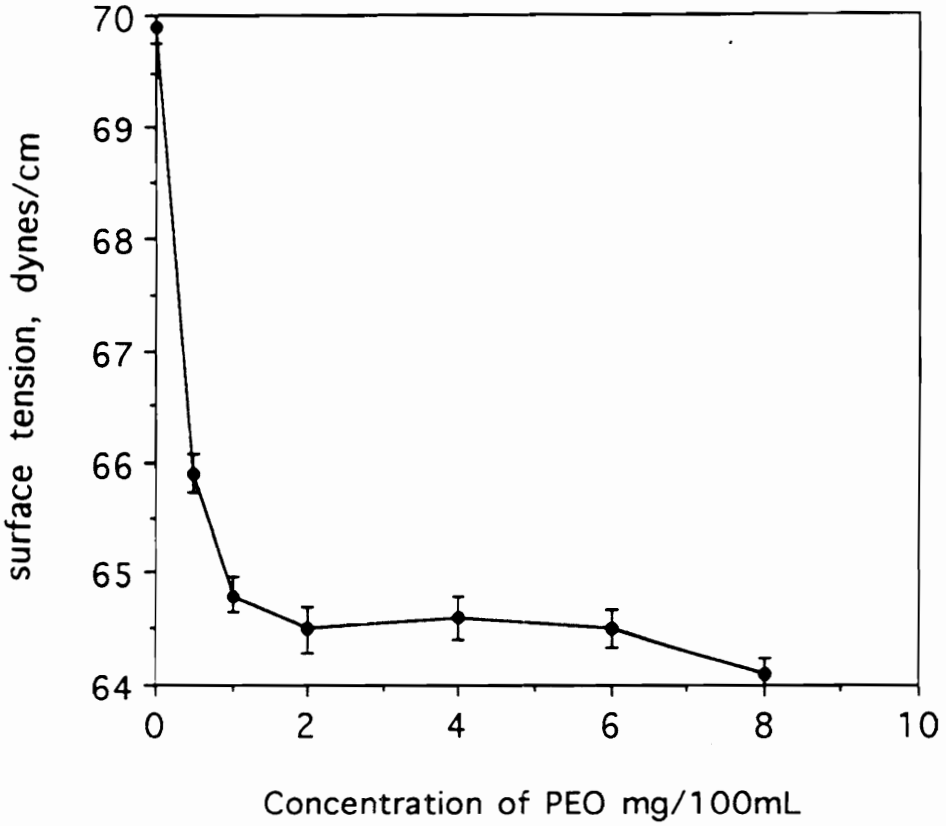

Figure 9. Effect of PEO on surface tension. Measurements taken at 26^0 C

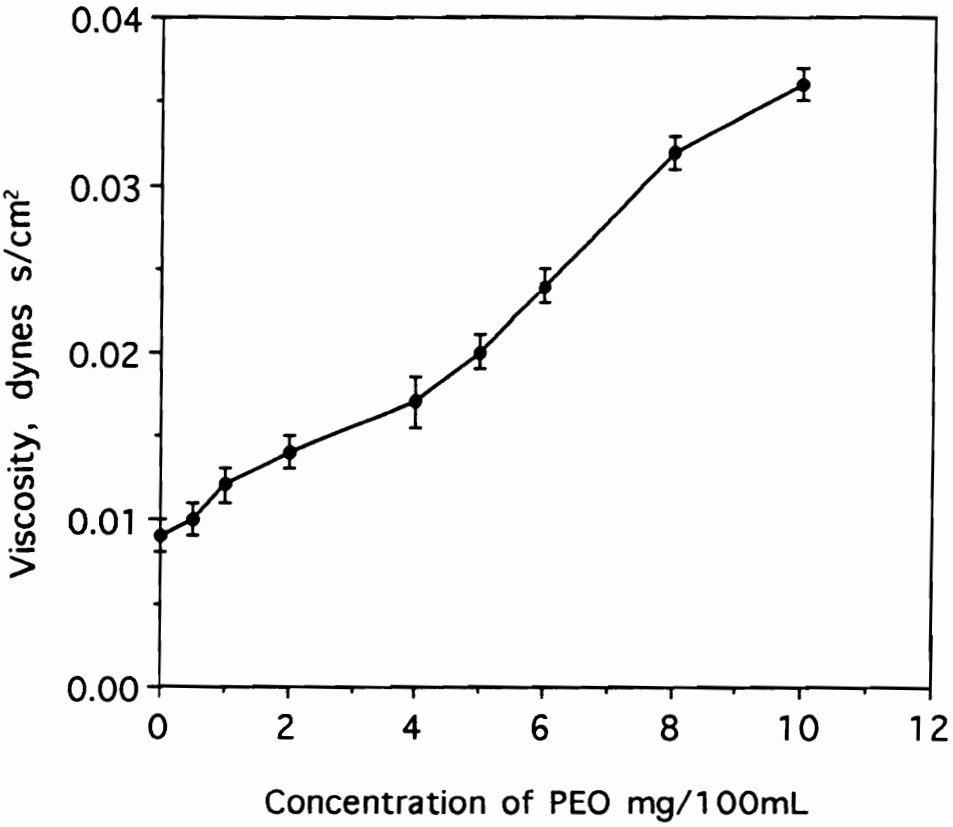

Figure 10. Effect of PEO on viscosity. Measurements were taken at 26° C

Table 4. Physical properties of slurries in Polyethylene oxide

PEO (mg/100 mL)	ρ **(g/mL)**	η **(dynes s/cm^2)**	γ**(dynes/cm)**
0.0	1.00	0.009	69.9
0.5	1.00	0.010	65.9
1.0	1.01	0.012	64.8
2.0	1.02	0.014	64.5
4.0	1.03	0.017	64.6
5.0	1.03	0.020	-
6.0	1.04	0.024	64.5
8.0	1.08	0.032	64.1
10.0	1.10	0.036	-

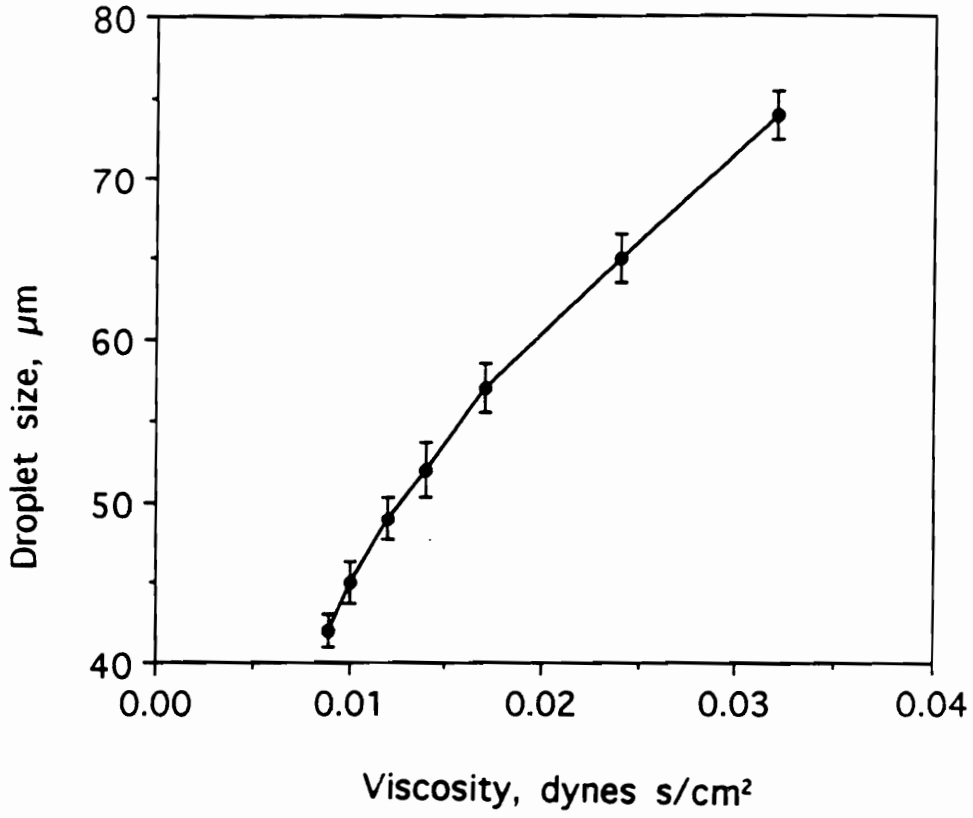

Figure 11. Effect of slurry viscosity on droplet size. The mean diameters were calculated using the Nukiyama-Tanasawa equation.

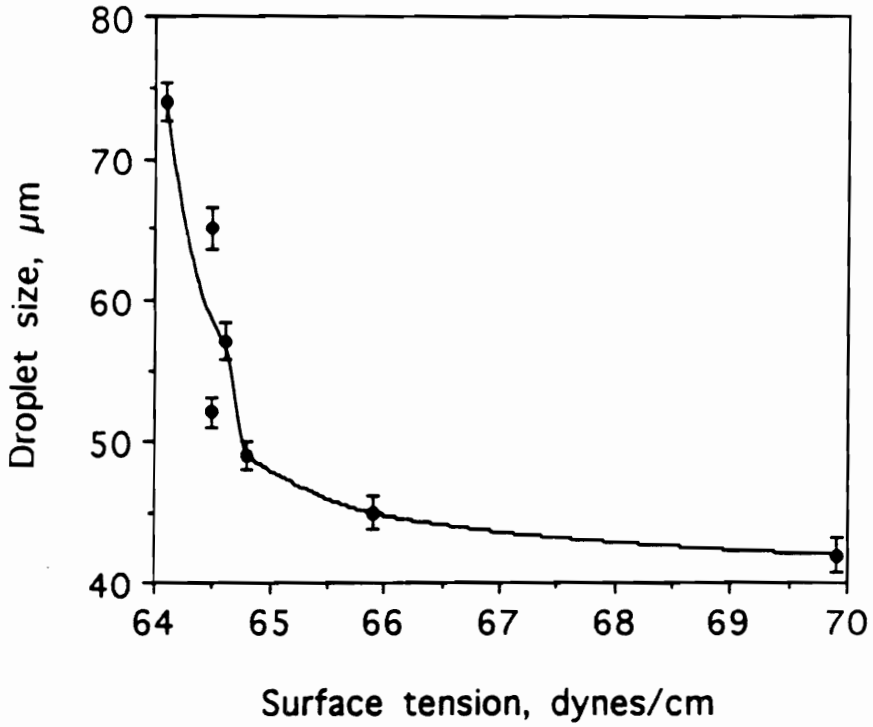

Figure 12. Effect of surface tension on droplet size. The mean diameters calculated using the Nukiyama-Tanasawa equation.

$$d_o = \frac{585}{V}\left(\frac{\sqrt{\gamma}}{\sqrt{\rho}}\right) + 597\left[\frac{\eta}{\sqrt{\gamma \times \rho}}\right]^{0.45}\left[1000 \times \frac{Q_l}{Q_g}\right]^{1.5} \quad (3)$$

where d_o = mean droplet size (μm)

V = velocity difference between gas and liquid ($v_g - v_l$) in m/s. Here, $v_g = Q_g/A_g$ and $v_l = Q_l/A_l$, Q_g and Q_l are flow rates of gas and liquid respectively. A_g and A_l are areas of gas and liquid tubes at the nozzle respectively

γ = surface tension (dyne/cm)

η = coefficient of viscosity (dynes s/cm^2) or poise

ρ = density of liquid (g/cm^3).

If gas and liquid flow rates are constant, then d_o depends only on density, viscosity and surface tension of the sample. Since the Nukiyama-Tanasawa equation was not derived for a Babington nebulizer (but for concentric nebulizer) the mean diameter derived is often overestimated [47]. The equation was developed for supersonic nebulizers, whereby the ratio $Q_l/Q_g = 10^{-6}$ [28]. In the present research this ratio was on the order of 10^{-3}. Despite this difference, the equation has been successfully used by some workers to predict trends for aerosol droplet size generated by nebulizers operating at subsonic gas flows. This prediction is possible as long as the experimental conditions are within the following limits: density, 0.8-1.2 g/cm^3; surface tension, 30-73 dynes/cm; viscosity, 0.01 - 0.3 dynes s/cm^2 [28, 47]. The size predicted for this type of nebulizer may be twice the actual size [38]. Broekaert *et al.* [19] have estimated that for a Babington nebulizer, V-grove type, the mean diameter of primary droplets is about 15 μm. The cut-off diameter

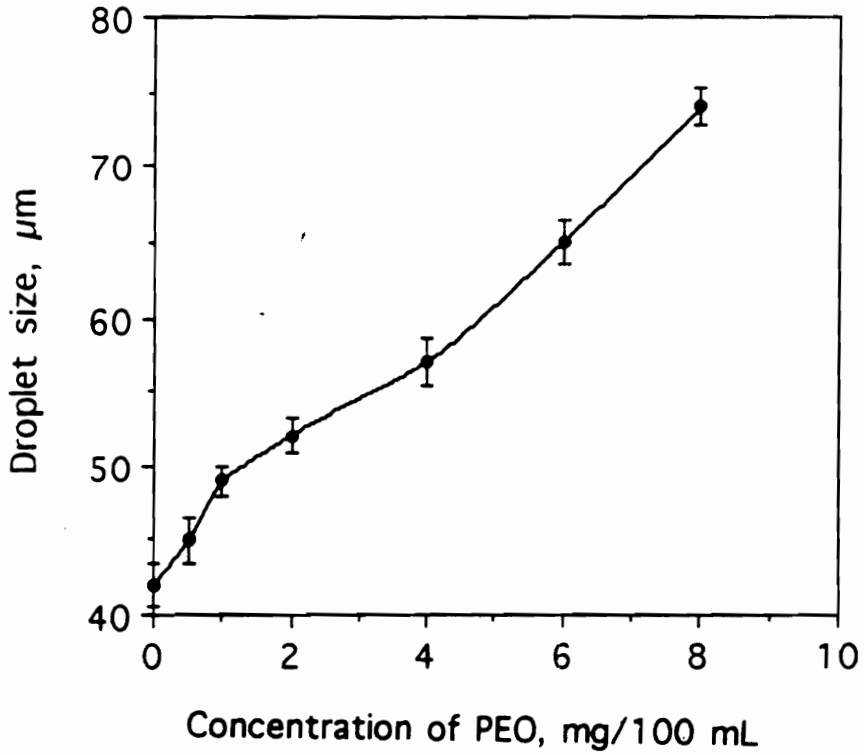

Figure 13. Effect of concentration of PEO on droplet size. This is a combined effect of surface tension and viscosity.

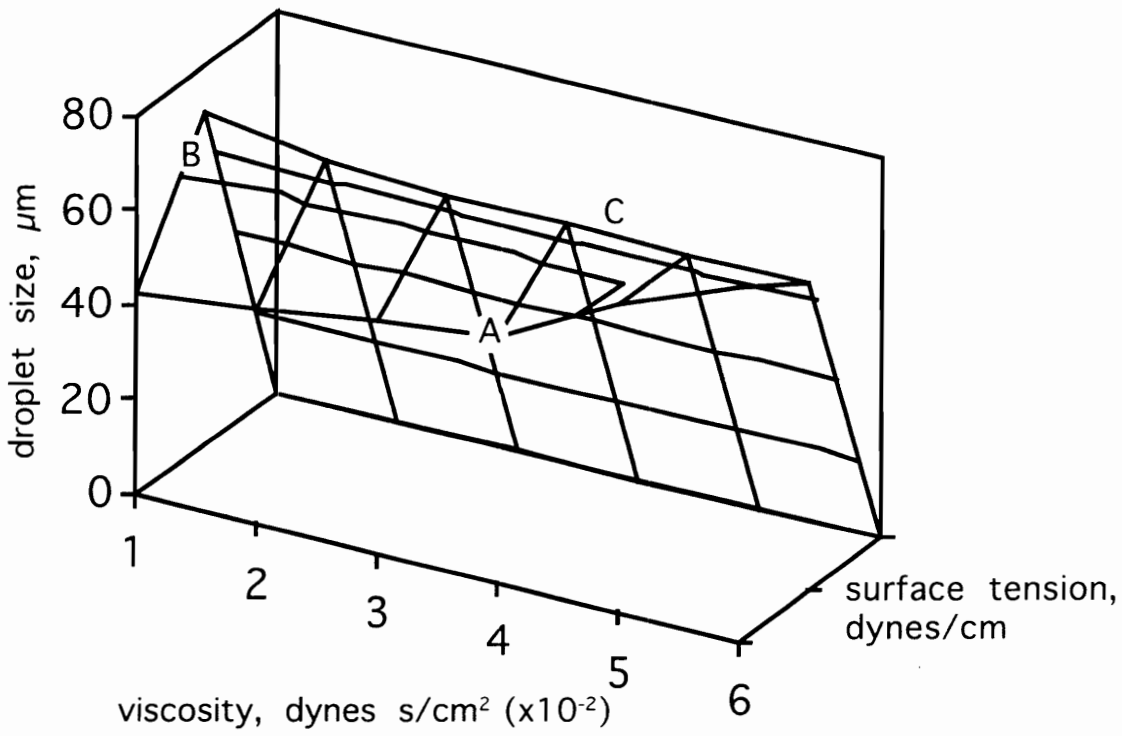

Figure 14. Effect of surface tension and viscosity of PEO on aerosol droplet size. (A = increasing surface tension; B = increasing droplet size; C = decreasing surface tension)

(D_c), *i.e.* of those droplets formed after impaction with the impaction bead, (secondary droplets) is smaller than this [28].

Practically, the effect of viscosity and surface tension on droplet size as calculated using the Nukiyama-Tanasawa equation is shown on Fig. 11 and 12 respectively. Figure 11 shows that indeed the droplet size increases with increasing viscosity. However contrary to expectations, Fig. 12 indicates that large droplets correspond to lower surface tension. These two observations lead to the conclusion that viscosity is more dominant than surface tension in determining the droplet size of slurries containing PEO that are produced by this nebulizer. This conclusion contradicts that reported by Kodama *et al.*[31] who studied the role of a surfactant, sodium dodecyl sulfate (SDS) in atomic absorption flame spectrometry. In that study, as surface tension was lowered by increasing the concentration of SDS, the mean droplet size was also lowered until the critical micelle concentration was reached, after which the droplet size remained constant. On the other hand, unlike PEO in this work, the viscosity of SDS solution in the previous study did not change significantly with concentration. Thus, according to results of the previous study, surface tension rather than viscosity was thought to be the predominant factor in determining the droplet size of aerosol. However due to the viscous nature of PEO (Figure 10), the present study has revealed the opposite effect. Figure 13 shows the effect of concentration of PEO on droplet size. This Figure is very similar to Figure 11 (viscosity - droplet). Since Figure 13 is a combination of the effect of both surface tension and viscosity, the similarity to only viscosity - droplet is an indication of the predominance of viscosity on droplet size. This conclusion was further supported by a three dimensional relationship between droplet size, viscosity and surface tension (Figure 14). Clearly, the droplet size increases as well as the viscosity while surface tension was decreasing.

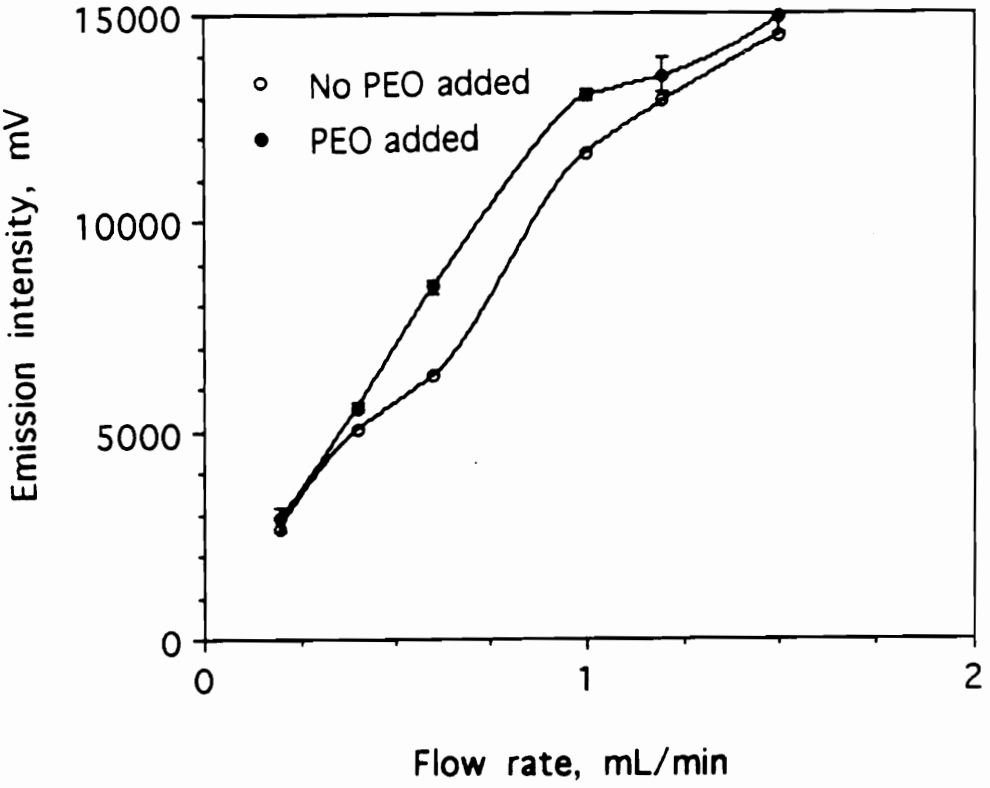

Figure 15. Effect of sample flow rate on emission signal (Al 396.15nm); with and without PEO. The enhanced signal in the presence of 5 ppm PEO is due to better nebulization efficiency which appears to be significant at medium flow rate, 0.6 - 1.0 mL/min.

Nebulization Efficiency: The enlargement of the mean droplet size explained above as being due to increased viscosity should result in a decrease in emission signal as a result of poor transport of large droplets (above D_c) into the plasma. However, a substantial enhancement of signal was observed at very low concentrations of PEO (Figure 8), and must result from some improvement in the nebulization process. This improvement can be rationalized by considering how a Babington nebulizer functions. The sample is pumped through a short glass delivery tube onto the outside surface of another hollow tube, the nebulizer tube, where it forms a thin film over the sphere. Both these tubes are typically 2 mm internal diameter. High velocity gas is forced through a small horizontal orifice in the nebulizer sphere, breaking the film into small droplets *i.e.* forming the aerosol. The presence of PEO and the consequent increase in viscosity causes the thickening of this film. Since the viscosity of a liquid has been described as a measure of the liquid's resistance to deformation rate [48], the thickened film has a higher residence time on the surface of the nebulizer tube. This allows for a better contact of gas with analyte than a thinner film from analytes without PEO. As a result of this phenomenon, more aerosol is produced in the presence of PEO than in the absence of it.

The data in Figure 8 show approximately a 50% increase in Al emission intensity with the addition of 5 ppm PEO to the slurry solution. A similar increase in emission for an aqueous Al solution was realized at this level of PEO. The similarity of enhancement of both slurry and solution indicate that the mechanism of signal enhancement at this low level of PEO must be an increase in the nebulization efficiency of the Babington nebulizer.

To demonstrate the formation of this liquid film, an experiment was performed in which the emission signal was monitored as a function of the analyte flow rate. Results of this study are presented on Figure 15. It was found that although the emission signal is generally higher for samples containing 5 ppm PEO than those without the surfactant, it

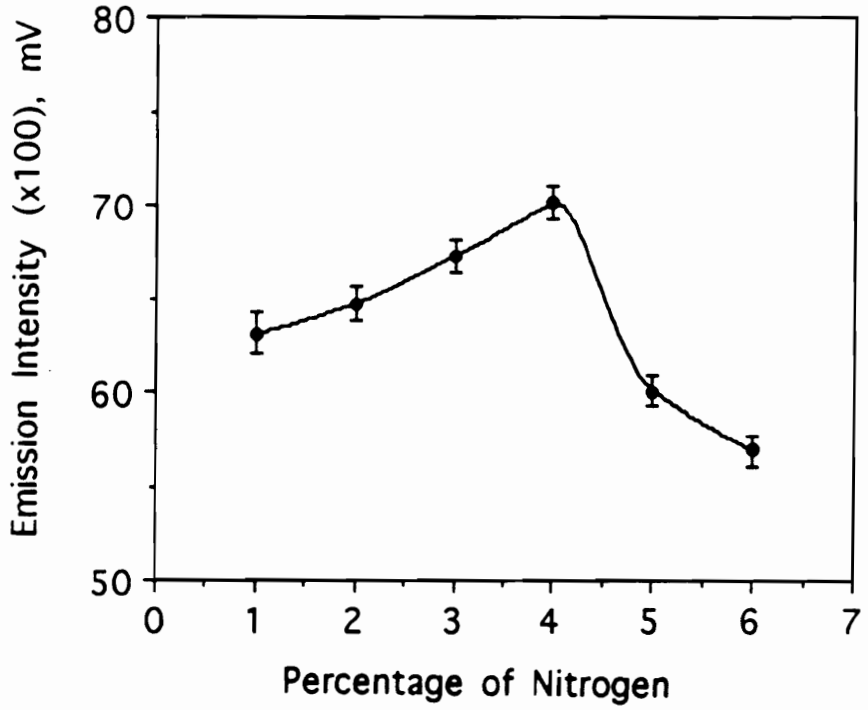

Figure 16. Effect of percent N_2 in cooling gas on emission intensity (Al 396.15 nm). The forward power was 1.25kW, observation height 10 mm above the induction coil.

appears that this difference is less significant at high flow rates (1.2 to 1.5 mL/min) and low flow rates (0.2 to 0.4 mL/min). However, at medium flow rates (0.6 to 1.0 mL/min) the difference is much more significant. This trend demonstrates that at high flow rates there is not sufficient time for a thicker film to build up, and despite the increased viscosity for PEO-containing samples, the efficiency of nebulization is not enhanced. As the flow is decreased to a medium rate, a thicker liquid film is formed on the nebulizer tube sphere. This translates into the formation of more aerosol and ultimately more signal compared to samples without PEO. At much lower flow rates, although a thicker liquid film may be formed in the presence of PEO, there is low analyte mass present on the surface at any particular moment. Thus the aerosol produced contains much less analyte for both samples with and without PEO. The overall trend of reduced emission as flow rates decrease underscores this point.

The effect of PEO concentration on emission signal presented in Figure 8 was obtained by introducing the sample at a medium flow rate of 1 mL/minute. The optimum concentration of PEO which caused this improved nebulization was 5 ppm. As the concentration of PEO was increased and consequently viscosity increased, the droplet sizes became too large. The ultimate effect was a sharp decrease in emission signal as shown in this Figure. Such large droplets undergo centrifugal and impaction losses to the walls of the spray chamber, and they also experience gravitational settling as they are transported through the spray chamber and into the plasma torch [19].

Effect of Mixed Gas Plasma: In an effort to improve atomization efficiency, mixed gas plasma was used instead of pure argon plasma. The effect of introducing small amounts of N_2 into the tangential cooling gas stream of an argon plasma is presented in Figure 16. The emission signal of Al at 396.152 nm from Al_2O_3 introduced into the

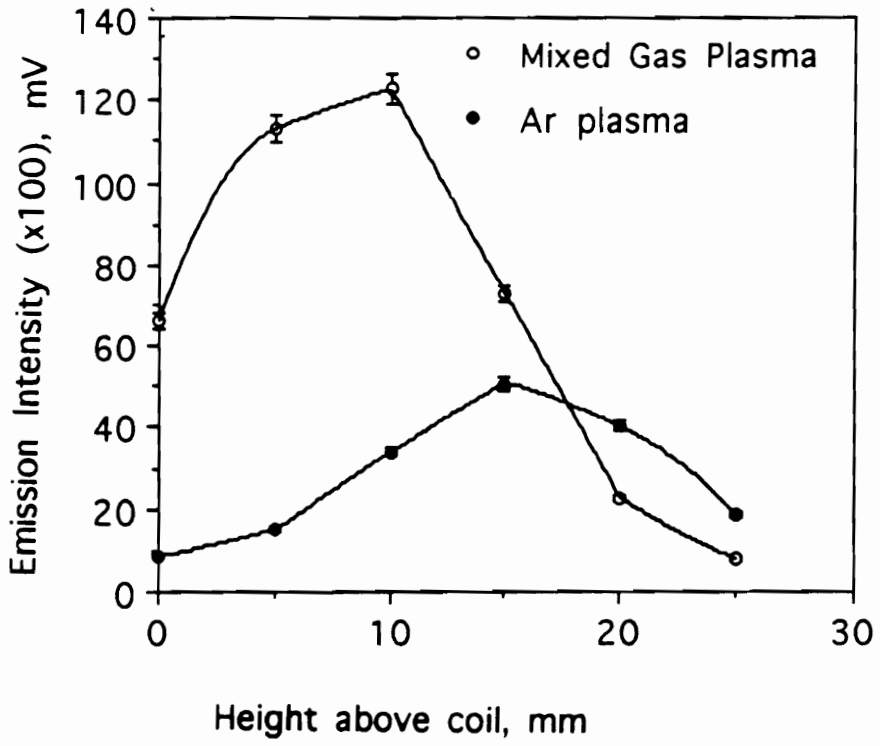

Figure 17. Comparison of mixed gas (4% N_2) with pure argon signals (Al 396.15 nm). Both emission profiles were obtained with a 1.25kW plasma. Reflected power for mixed gas was about 25 watts, whereas for argon plasma it was < 10 watts.

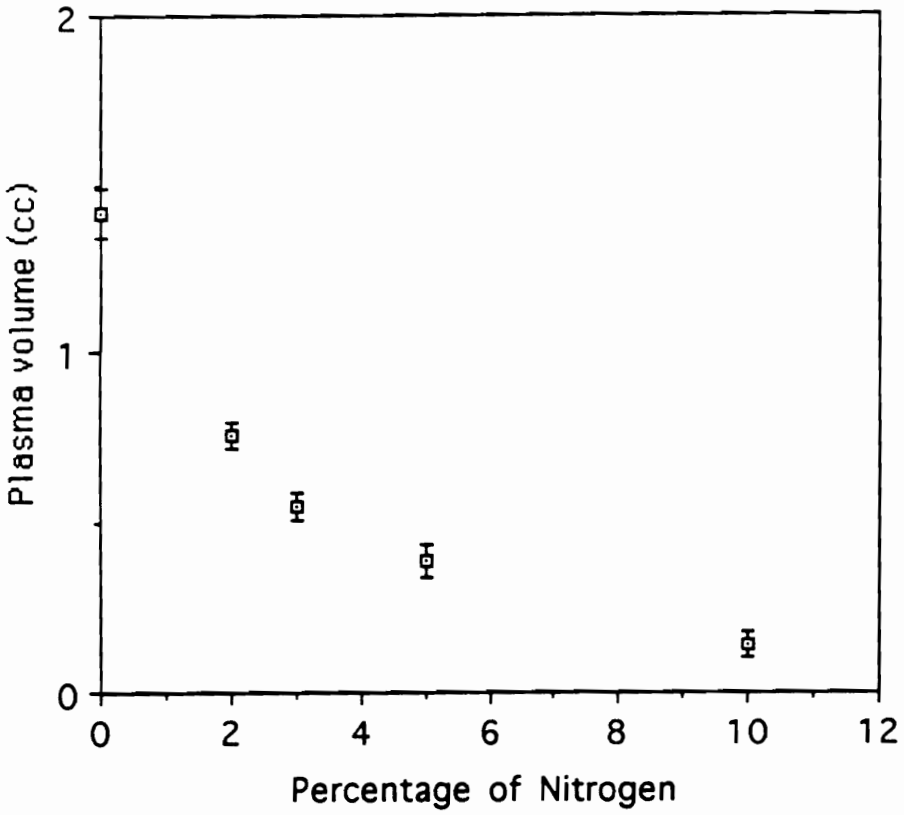

Figure 18. Effect of nitrogen on plasma volume: Thermal pinch.

plasma increases with flow rates of N_2 that comprise up to 4% of the cooling gas flow. Further increases in N_2 flows result in an unstable plasma and a high background emission signal. Thus, 4% N_2 was used in all the experiments involving mixed gas plasma. An emission profile for pure argon and Ar/ 4% N_2 (Figure 17) indicates two important features: 1) the point of maximum emission for the mixed gas plasma with slurry nebulization is lower (10 mm above the coil) than for pure argon (15 mm) and 2) the ratio of emission signal from mixed gas and pure argon, was 3:1 respectively. These observations can be explained by studying the changes which take place in the plasma as a result of the presence of nitrogen.

Plasma Thermal Pinch: In Chapter 1, it was noted that the presence of N_2 constricts the discharge (thermal pinch) and results in a higher energy density in the central channel of the plasma, where the analyte undergoes atomization [9, 49, 50]. Capitelli *et al.* [14] have reported the thermal conductivity of three plasmas; Ar, Ar + 4%N_2 and Ar + 8%N_2. At 6000 K, which is the approximate temperature of plasma at the viewing height, it is 25, 90 and 140 Kcal/cm respectively. The same authors calculated the amount of heat transferred to a 60 μm particle of Al_2O_3 moving through plasma. On the basis of these results, other conditions being equal, a 60 μm Al_2O_3 particle traveling across the plasma should receive about 80% more heat in an Ar + 8% N_2 than pure argon plasma.

The constriction of the plasma discharge, was quantitatively measured as a function of concentration of molecular gases (nitrogen and hydrogen). Direct measurement of the plasma height and width was performed. The plasma volume was then calculated assuming that it has a conical shape, with the formula $V = 1/3(\pi r^2 h)$, where r is the radius of the base of the cone and h is its height perpendicular to the base.

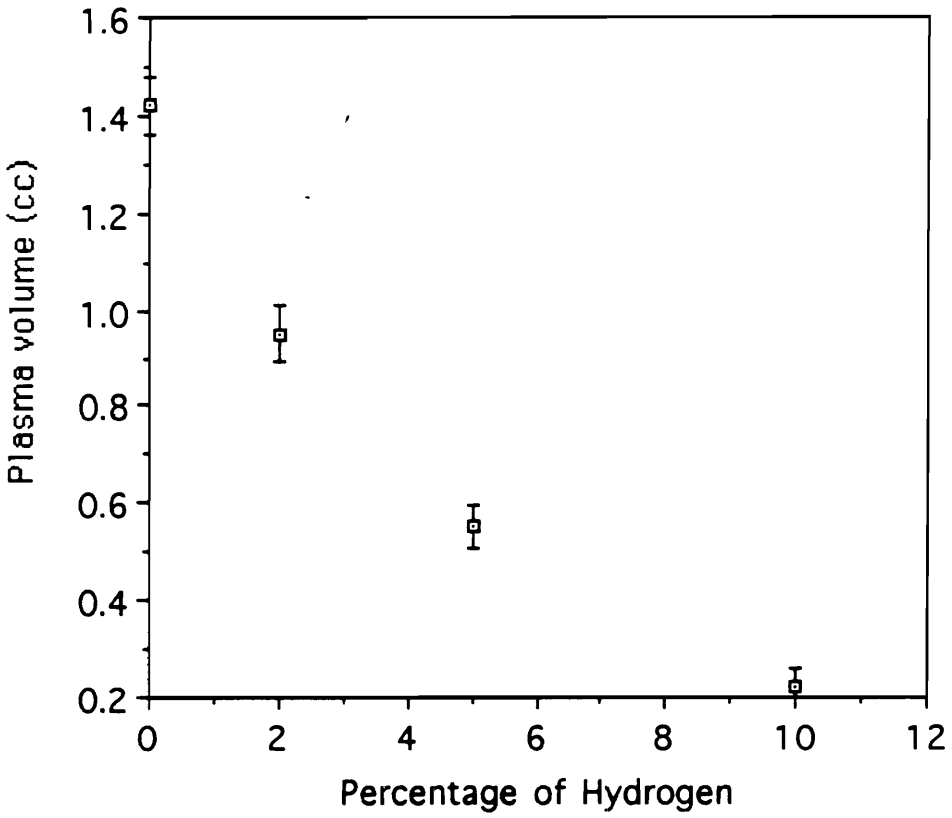

Figure 19. Effect of hydrogen on plasma volume: Thermal pinch.

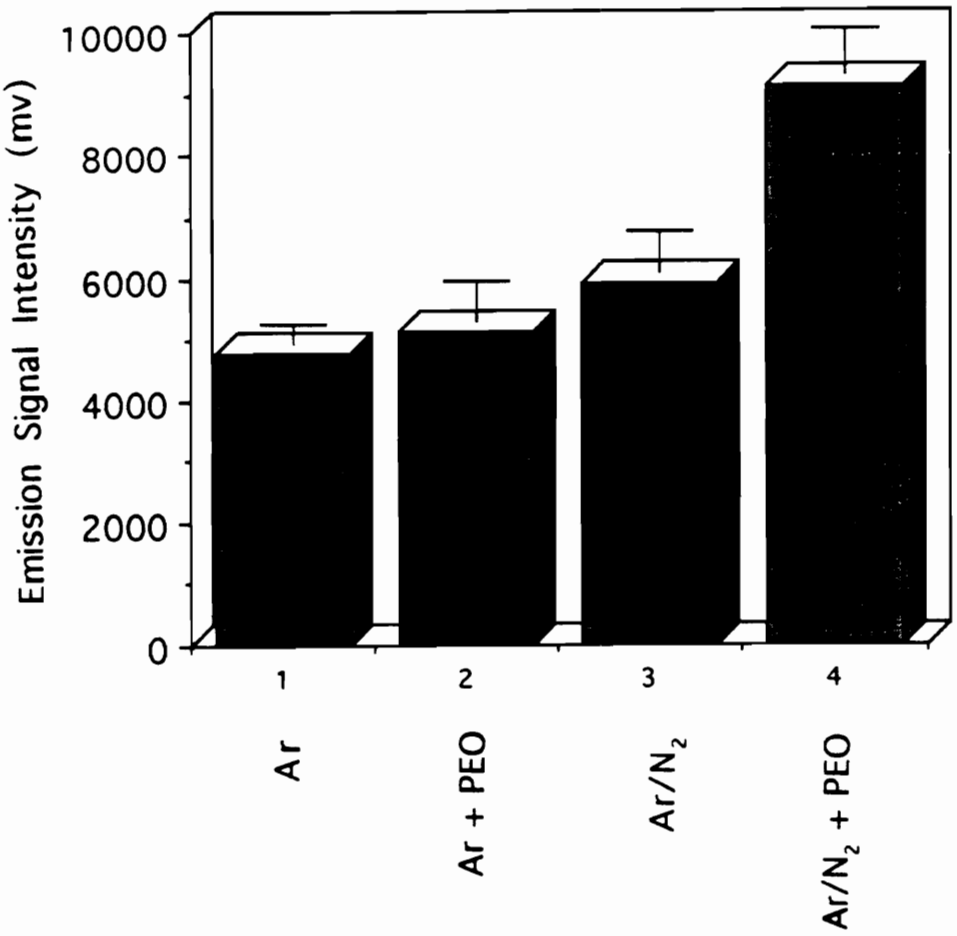

Figure 20. Summary of data for mixed gas (4% N_2) vs pure argon in the presence and absence of 5 ppm PEO. The sample for this comparison was 0.1% m/v alumina slurry. The emission line was Al 396.15 nm.

Table 5. Comparison of N_2 and H_2 on plasma volume pinching.*

% N_2 and H_2	Volume with N_2	Volume with H_2	V_{N2}/ V_{H2}
0	100	100	1
2	54	68	0.8
5	27	39	0.7
10	10	16	0.6

* All volumes are in cm^3

The total flow (Ar + N_2 or H_2) was 15 L/min.

The dimensions of the plasma were taken by placing a piece of paper on the outside of the UV - protected glass window of the torch box. By sketching the bright plasma discharge, it was possible to measure its height and width.

Figures 18 and 19 show how the plasma volume varies with increasing amount of nitrogen and hydrogen in the cooling gas stream, respectively. It is evident from the figures that, the introduction of just 2% nitrogen results in plasma volume reduction to 54%. At 5% nitrogen, about which maximum emission occurs, the plasma has been reduced to 27% of the original volume. The addition of 10% nitrogen leads to a plasma that is only 10% of the original volume. By comparison, the presence of hydrogen shows less pinching effect than nitrogen. A comparison of the two figures is presented on Table 5, where the ratio of plasma volume remaining at each percent gas is given. For 2% gas, $V_{nitrogen}/V_{hydrogen}$ is 0.8; 5% is 0.7; and 10% gas, the ratio is 0.6. The latter ratio indicates that, the size of the plasma remaining after adding 10% nitrogen is about half the size remaining after adding the same amount of hydrogen.

The difference between the effect of these two molecular gases on plasma thermal pinching can be explained in terms of their differences in thermal conductivity. Nitrogen has a relatively higher thermal conductivity than hydrogen at all temperatures. The ratio of their thermal conductivity is about 14 [46]. In this connection, it is important to understand why thermal pinch occurs, in terms of thermal transfer. Assuming that a plasma is a hot cylindrical tube (the torus) through which flows a gas, a simple heat - transfer mechanism can be assumed to be taking place. Thermal pinch results from the fact that, the increased heat transfer from the surface skin of the plasma leads to contraction of the plasma torus in order to maintain charge carrier density and therefore conductivity of the skin [15]. In other words, heat transfer takes place from the hotter

outer surface, where there is high conductive molecular gases, to the cooler inner portion of the plasma.

There are two consequences of this contraction; first, the geometric contact area decreases and second the residence time of gases or analyte in the axial (central) channel is decreased as gas velocities are increased by the smaller channel diameter. Indeed, Ebdon and associate [15] have reported that, the residence time of gas and/or analyte in the central channel is proportional to the square of the radius of the central channel. Thus, if t is the residence time of gas or analyte and $\boldsymbol{r}$ the radius of the central channel then, the two are related as follows:

$$t = k\, r^2 \tag{4}$$

where k is the proportional constant. This simply implies that, if the axial radius were reduced by a factor of 2, the residence time would consequently be reduced by a factor of4.

The gas velocity is further increased (hence residence time further decreased) by the increased temperature as a result of the heat transfer from the plasma skin. The replacement of argon with molecular gases and hence the increase of temperature, however has been described by Ebdon [15] as being self limiting. This is because it decreases the residence time and therefore limits the effect of increased thermal conductivity. This self limiting effect has been demonstrated in the present study by the shape of Figure 15 (*i.e.* emission signal versus concentration of nitrogen). This figure shows some steady increase of temperature to a certain level, then a sharp decrease with concentration of the molecular gas. The decrease is a consequence of reduced residence time of analyte in the central channel. This observation is similar to that reported by Ebdon [15].

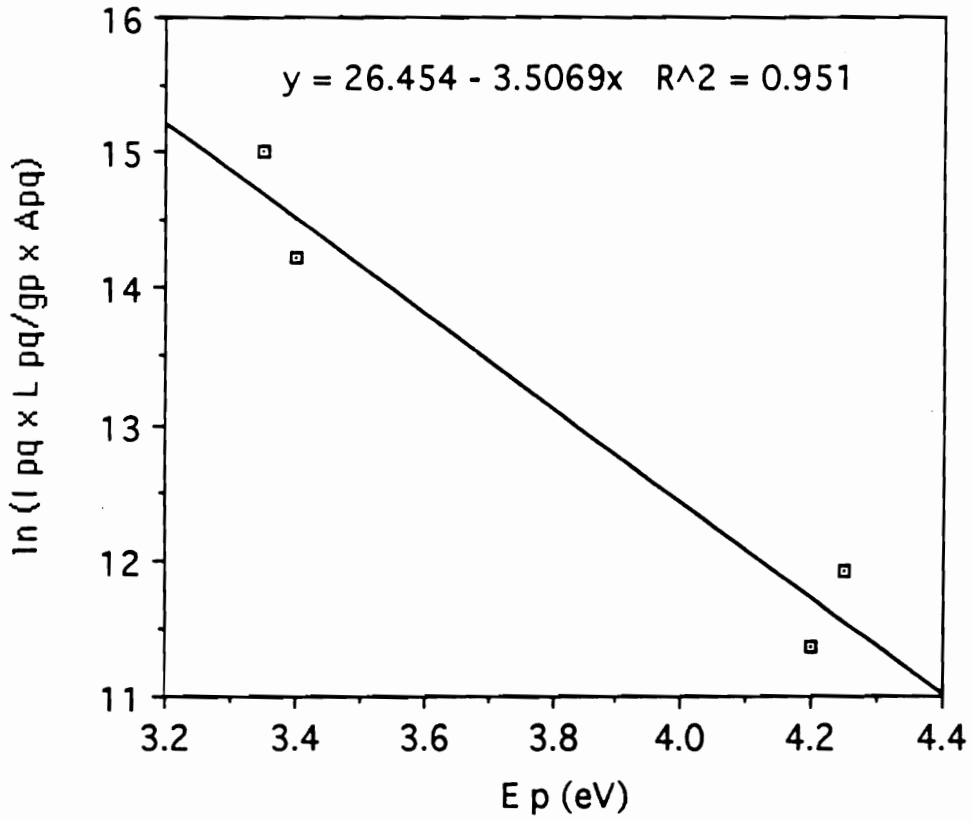

Figure 21. Boltzmann Plot: Excitation temperature measurement using Fe.

As noted in the review articles in Chapter 1, when molecular gases were introduced into the injector (nebulizer) gas stream, the following observations were made: the plasma height decreases but not as much as it does when the gases are in the cooling stream; and the axial channel expands significantly. Although it was not practically possible to quantify the expansion of the central channel, yet another important observation was made and that is, the external diameter of the torus remained virtually unchanged. As a result of this, the toroidal thickness is significantly reduced. The addition of more than 50% molecular gas, *i.e.* in excess of 1.5 L/min (equivalent of 10% in the outer flow) extinguishes the plasma due to the collapse of the torus. This observation is similar in both nitrogen and hydrogen injection.

Figure 20 summarizes the dual effect of PEO and mixed gas on the emission of aluminum from aluminum slurries. The mean signal intensity for each plasma is displayed in a bar graph format. The 95% confidence interval of error in signal from each data set is indicated with the associated error bar. In the presence of nitrogen, the emission signal from slurries with PEO is 35% higher than that obtained from samples without PEO (3^{rd} and 4^{th} bar). On the other hand, in the absence of nitrogen, this difference is just about 10% (1^{st} and 2^{nd} bar) for this particular sample, 0.1% m/v slurry, that is 0.1 g Al_2O_3 and 99.9 mL water. The difference between mixed gas plasma emission and pure argon emission in the presence of PEO is 43% (2^{nd} and 4^{th} bar) and only 20% in the absence of PEO (1^{st} and 3^{rd} bar). This figure shows that the positive effect of PEO is further augmented by the use of a mixed gas plasma.

Summary: Data presented in this chapter have demonstrated that the addition of a controlled amount of non-ionic surfactant, polyethylene oxide, to aqueous alumina slurries, significantly enhances the emission signal of aluminum. Unlike other surfactants,

the enhancement of emission signal does not seem to be caused by improved transportation resulting from reduced droplet size of the aerosol. It appears that the presence of PEO in the slurries, and consequently elevated viscosity, provides efficient nebulization. This improved nebulization results in enhanced emission signal at small levels of PEO. However, the signal is drastically reduced with further addition of PEO due to the formation of large droplets. The use of mixed gas plasma further increases the intensity of the emission signal, although this effect is self-limiting. About 4 % to 5% nitrogen seems to be the optimum amount. It is suggested that slurries of larger mean particle diameter than recommended in previous studies could be efficiently analyzed by this technique.

Chapter 4

OPTIMIZATION OF PLASMA CONDITIONS: TEMPERATURE MEASUREMENTS

Introduction: To evaluate the capability of a spectrometric method, a number of diagnostic measurements are normally performed. For plasma sources, temperature and electron number density are routinely measured. Excitation temperature and rotational temperatures are conveniently determined to characterize inductively coupled plasmas. The rotational temperature of a mixed gas plasma such as Ar/N_2 is particularly convenient to measure because N_2^+ gas is also used as the thermometric species. Both excitation and rotational temperatures describe the suitability of a plasma for emission spectrometry. Temperature values for plasmas consisting of pure argon and argon with small amounts of nitrogen or hydrogen are obtained and compared to determine the optimum conditions, in terms of amount of molecular gas to be mixed and height above the induction coil in the plasma. The difference between mixing molecular gases with argon in the cooling gas and in the injector gas is also explored. This chapter describes the theory and procedure of the temperature measurements, compares values obtained using different thermometric species and attempts to explain the differences.

Data from excitation temperature measurements is also used to predict the mechanism of vaporization. The use of Fe as a thermometric species from solution and slurry sources is particularly helpful for mechanism studies. Fick's laws of diffusion have been employed for this study.

Excitation Temperature: Excitation temperature is a measure of the energy available for excitation of analyte species. The method routinely used to determine excitation temperature of the plasma is the slope method using the relative emission intensities of Fe lines [12] as the thermometric species. An iron solution of 1000 ppm is introduced into the plasma and the relative intensities of the iron atom lines within the spectral region 370-390 nm are measured. In this project, in addition to solution introduction, for comparison purposes, iron was also introduced as Fe_2O_3 slurry. In this case 0.14 g of the oxide (mean particle diameter <5 μm) was mixed with 100 mL of distilled-de ionized water. This slurry contains 0.1 g Fe in 100 mL or 1000 mg/L which is equivalent to 1000 ppm Fe. By assuming a Boltzmann distribution of excited states, the following equation can be applied [51].

$$\ln\left[(I_{pq} \times lpq) / g_p \times A_{pq}\right] = E_p / k \times T_{exc} + \text{constant} \qquad (5)$$

where:

I_{pq} = measured relative intensity

l_{pq} = wavelength of the emission line

g_p = statistical weight of the upper state, p

A_{pq} = transition probability for spontaneous emission

E_p = energy of the upper state, p

k = Boltzmann constant, $1.3806*10^{-23}$ J/K or $8.617*10^{-5}$ eV/K

T_{exc} = excitation temperature (electronic transition temp.)

The left hand side of the equation is plotted against the energy of the upper (excited) state, E_p for a number of atomic lines (normally between 3 and 10). In this study, 6 lines with wavelengths between 367.992 nm and 376.379 nm were selected. The other

Table 6. Spectrometric constants of Fe used for determination of excitation temperature

Wavelength (nm)	**E_p (cm^{-1}) [(eV)]**	**g_p**	**A_{pq}**
367.992	27167 [3.35]	9	0.014
371.994	26875 [3.30]	11	0.163
372.256	27560 [3.40]	5	0.051
373.487	33695 [4.15]	11	0.886
375.824	34329 [4.20]	7	0.611
376.379	34547 [4.25]	5	0.523

E_p = energy of the upper state

g_p = statistical weight of the upper state

A_{pq} = transition probability for spontaneous emission

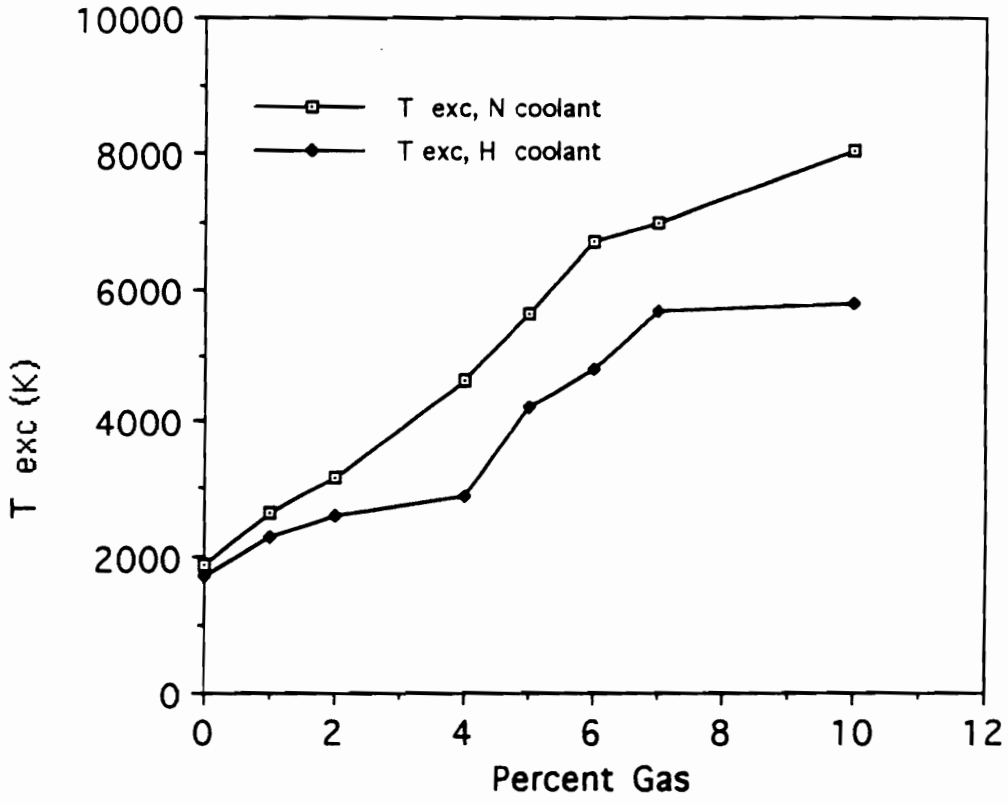

Figure 22. Comparison of T_{exc}; N_2 and H_2 in cooling gas. Thermometric species: Fe in Fe(II) solution.

constants of the equation are listed in Table 6 [52]. A typical plot is shown in Figure 21, which has a slope inversely proportional to the excitation temperature. From the slope of the curve (- 1/kT), the excitation temperature T is calculated. Since the Boltzmann constant is used in eV/K, before plotting the graph it was necessary to change all E_q from cm^{-1} to eV [53]. Manual calculation of the product of the left hand side of the equation can be performed or simply the wavelength and intensity data is entered into a computer program whereby T_{exc} is calculated via linear regression [54].

Excitation temperatures were determined for plasmas containing either N_2 or H_2 in the injector gas or in the cooling gas stream.

Effect of N_2 and H_2 in the Cooling Gas: When small amounts of molecular gases are mixed with argon in the outer or cooling stream, it was demonstrated in Chapter 3 that the emission capability of the plasma is significantly improved. Measurements of excitation temperature of these plasmas should help to explain the phenomenon. Figure 22 compares the effect of small amounts of nitrogen and hydrogen gas in the cooling gas stream. The data were obtained at 10 mm above coil since this was the optimum position for 4% N_2, the concentration around which maximum emission was obtained (Figure 16). The consequence of collecting signal at 10 mm instead of 15 mm, however is that an abnormally low excitation temperature is recorded for 0% nitrogen and hydrogen. It should be recalled that with pure argon, the optimum emission height is 15 mm (Figure 17). This height was not used here because the interest of this part of the study was the emission of mixed gas not pure argon. Thus, the conditions have to be optimized to suit mixed gas emissions. The excitation temperature increases with increasing percent nitrogen and hydrogen. This increase tends to level off at around 6% for nitrogen and 7% for hydrogen whereby the temperature is about 7000 K and 5500 K, respectively. The

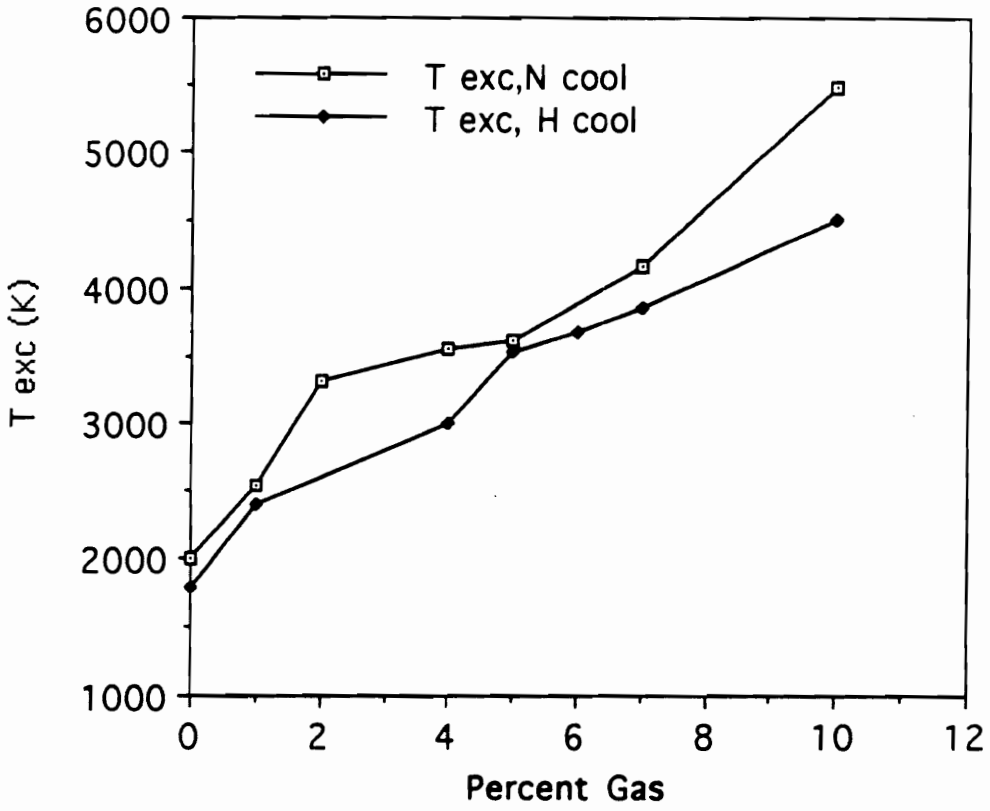

Figure 23. Comparison of T_{exc}; N_2 and H_2 in cooling gas. Thermometric species: Fe in Fe(III) oxide slurry.

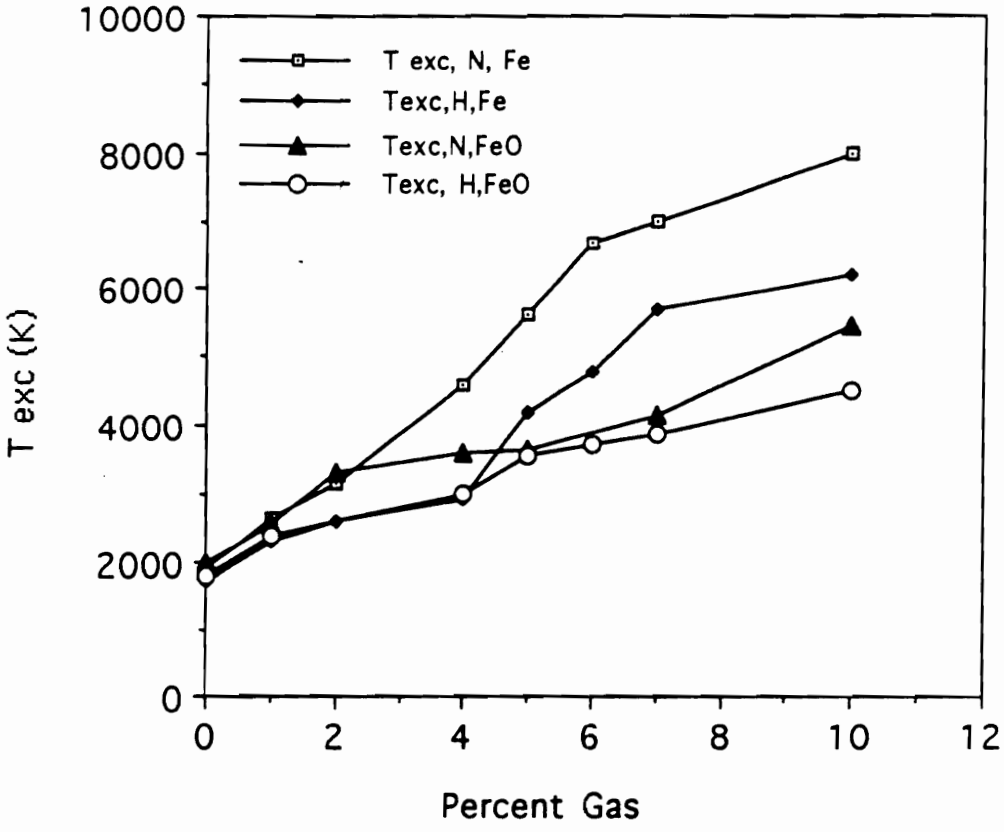

Figure 24: Effect of solution/slurry on T_{exc}. (Figure 22 and 23 compared)

figure also shows that there is a consistently higher temperature associated with the presence of nitrogen than hydrogen at all gas concentrations. This difference between nitrogen and hydrogen is attributed to the differences in their thermal conductivity which is in the ratio 14:1, nitrogen:hydrogen respectively, as was indicated earlier [48].

The phenomenon that a greater excitation temperature is obtained after 4% nitrogen or hydrogen cannot easily be explained, because this does not correspond to emission data (Figure 17) where emission diminished above 4 % nitrogen. In other words, T_{exc} unlike emission intensity or T_{rot}, does not seem to show the self-limiting effect described in Chapter 3. The phenomenon can be explained by exploring the Boltzmann distribution law which expresses the relation between temperature and the ratio n_q/n_o of the concentrations of atoms in the excited (q) and the ground state (o) [53]. The law can be written as :

$$n_q / n_o = (g_q / g_o)^{Eq/kT} \qquad (6)$$

where,

n_q = concentration of particles in excited state q

no = concentration of ground state atoms

g_q = statistical weight of the excited state

g_o = statistical weight of the ground state

E_q = excitation energy of the state q

k = Boltzmann constant

T = absolute temperature

The ground state population (n_o) declines with increasing temperature. The continued

depletion of the ground state causes the populations of high levels to rise with temperature.

Thus as the thermal conductivity of the plasma increases with increasing amount of nitrogen or hydrogen in the plasma, more and more gas species become excited as they absorb the thermal energy. Consequently the ratio n_q/n_o increases. According to the equation representing the Boltzmann distribution, the excitation temperature, T must increase. However, temperature increases even after the optimum nitrogen or hydrogen, unlike the emission plot (Figure 16) because the ratio n_q/n_o increases even after the optimum gas concentration.

Perhaps some of the excitation energy is lost during the collision process. It has been demonstrated [53] that the greater part of excited states will be lost in the so called "collisions of the second kind" whereby excited states are destroyed and no radiation is emitted, *i.e.* only a small fraction of the atoms involved is likely to give up excitation energy as emission of light quanta. This explains why a high excitation temperature does not necessarily corresponds to a high emission signal. The apparent loss of emission is observed in the presence of elevated concentration of molecular gas (above 4%). When an excited atom and a molecule collide, the excitation energy of the atom is easily passed on to the molecule. For a diatomic gas such as nitrogen or hydrogen, the energy is absorbed as rotational or vibrational energy, therefore this type of collision involves high efficiency for collision of the second kind in which excitation energy of atoms is converted into another form of energy but not into light energy. It is logical to infer that, the higher the concentration of the molecular gas, the higher is this loss of energy.

When the Fe_2O_3 slurry was used as a source of Fe, a similar trend was observed like when using an aqueous source as presented in Figure 23. However, less T_{exc} is recorded from slurry than from solution source of Fe for both nitrogen and hydrogen

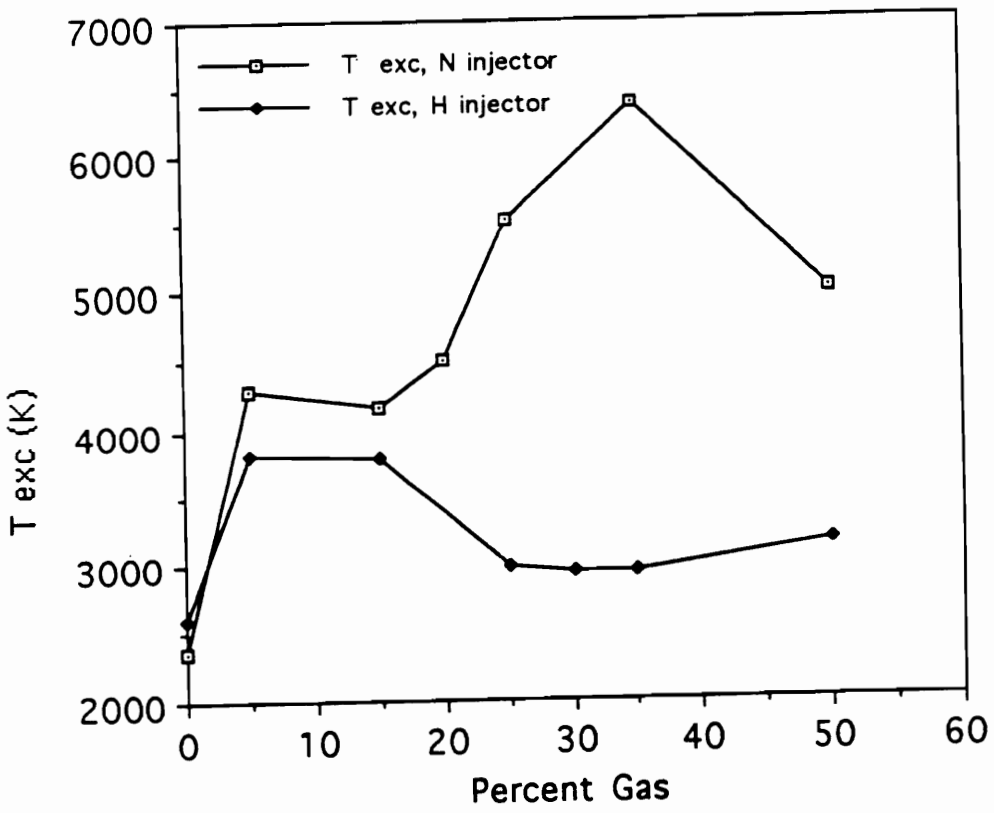

Figure 25. Comparison of T_{exc}; N_2 and H_2 in injector gas. Thermometric species Fe in Fe(II) solution.

gases. About 5500 K and 4500 K were obtained in the presence of N_2 and H_2, respectively when slurry was used compared to about 8000 K and 6000 K when solution was used. The two matrices are compared in Figure 23. The difference between T_{exc}. data from slurry and from solution can be attributed to the fact that some of the energy is used to break down and vaporize the refractory particles of Fe_2O_3 before they are atomized and excited. It is important to note that this data just like solution data were obtained at 10 mm above induction coil. Since this is not the optimum height above coil for 100% argon, the excitation temperature is unusually low, around 2000 K.

Effect of N_2 and H_2 in the Injector Gas: Several researchers have attempted to mix molecular gases with argon in the injector gas, *i.e.* the nebulizer gas stream. In these previous studies, there have been mixed and, sometimes conflicting results. While Ebdon *et al.* [15] and Meeks *et al.* [42] have reported significant enhancement in rotational temperature with the presence of hydrogen in the injector stream, Abdallah and associate [55], Northway *et al.* [56], and Montaser *et al.* [17], did not report any benefit in terms of emission signal, from mixing nitrogen with argon in the injector tube.

In this study, the excitation temperature was determined in the presence of nitrogen and also hydrogen. In order to rationally compare data for the two modes of mixed gas introduction, it was necessary to introduce the same amount of molecular gas for both systems. Since the total injector gas was only 3 L/min, whereas the cooling gas was 15 L/min, and if equal amounts of the diatomic gas are to be introduced in both cases, the percent nitrogen and hydrogen in the injector gas is 5 times the percent in the cooling gas stream. These amounts are presented in Table 7. Thus 50% nitrogen or hydrogen in Figure 25 (injector) is equivalent to 10% in cooling gas. Both these are 1.5 L/ min.

Table 7. Amounts of N_2 and H_2 introduced as cooling and injector gas

L/min	% Coolant (Total 15 L/min)	% Injector (Total 3L/min)
0.15	1	5
0.30	2	10
0.45	3	15
0.60	4	20
0.75	5	25
0.90	6	30
1.05	7	35
1.20	8	40
1.35	9	45
1.50	10	50

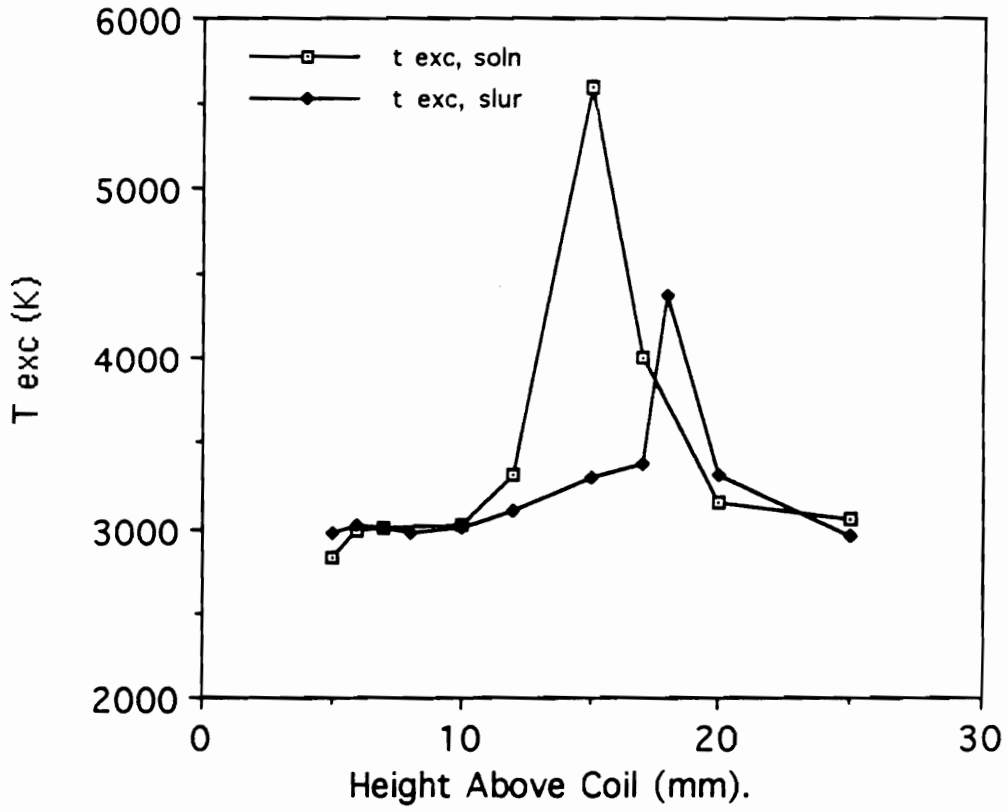

Figure 26. Excitation temperature profile for solution and slurry samples. Pure Argon plasma.

Figure 25 shows that T_{exc} tends to increase steadily with the addition of about 5% for both nitrogen and hydrogen and then levels off until 15% is added. After this, nitrogen plasma shows another relatively sharp increase up to 40% to a value of about 6500 K before it drops again. On the other hand, the hydrogen-containing plasma shows a decline of T_{exc} after 15% hydrogen has been added. There is a tendency of leveling off at around 3000 K between 25% and 50% hydrogen.

While the leveling and decline cannot be easily explained other than plasma instability as it was evidenced with axially introducing these gases (especially hydrogen), the decline of T_{exc} with nitrogen gas at 6500 - 7000 K is what would be expected. Based on literature cited in Chapter 1, the thermal conductivity of nitrogen increases with temperature up to about 6500 K, and declines above this temperature before it increases sharply at 9000 K. [13]. It is interesting to notice that this decline phenomenon was not observed in the cooling gas mixing (Figures 22 and 23). However, even in those situations, there was some tendency to level off at around 6000 - 6500 K. This shows that above this temperature the thermal conductivity and hence the excitation temperature does not increase as fast as before.

Excitation temperatures, determined under various experimental conditions including nature of molecular gas added and mode of introducing it, may be easily compared in a summary in Table 8. Only temperatures obtained upon addition of 0.6 L/min and 1.35 L/min are reported. These represent maximum emission environment (Chapter 3) and maximum amount of gas that was added, respectively.

Excitation Temperature Profiles: In atomic spectrometry, profiles are used to map out the spatial distribution of a measured parameter of the source. For the excitation temperature profile of a plasma, this entails the measurement of T_{exc} along the height of

Table 8. Excitation temperature measurements summary†

Plasma	**Temperature (K)***	
	0.6 L/min gas	*1.5 L/min gas*
Ar - N_2 cooling	4600 (150)‡	8020 (270)
Ar - N_2 injector	4500 (130)‡	5000 (120)
Ar - H_2 cooling	2890 (50)	5800 (120)
Ar - H_2 injector	3790 (100)	3150 (80)

* Errors in parenthesis.

† Thermometric species, Fe in Fe(II) solution.

‡ Not statistically different

plasma above the induction coil. Such vertical profiles are useful to determine the optimum height of observation above the coil under the prevailing experimental conditions. The instrument has a built-in device capable of changing the distance of observation above the coil.

For this study, it was desired to determine T_{exc} profiles using not only iron solution but also iron (III) oxide slurry in argon plasma. Another set of experiments was performed with 4% Ar/N_2 plasma which yielded the optimum emission signal (Figure 16). Figure 25 compares two T_{exc} profiles; the thermometric species Fe, introduced as solution and as a slurry in a pure argon plasma. Two distinctive features are demonstrated in this plot. With solution analyte, a higher temperature is realized than with slurry analyte. There is a difference of about 1400 K. The points of maximum temperature are 15 mm and 18 mm for solution and slurry, respectively. When 4% nitrogen was added, the point of maximum observation for both solution and slurry was lowered, and the highest temperatures in both cases were increased as follows: The solution observation height decreased from 15 mm to 10 mm, temperature increases from 5605 K to 6250 K (12% increase in T_{exc}.). Slurry observation height decreased from 18 mm to 14 mm, and temperature increases from 4366 K to 5201 K (20% increase). These are the direct consequences of a mixed gas plasma, which tends to be smaller but more energetic.

The two effects of mixed gas plasma, namely increased excitation temperature and lowered point of highest excitation, can be explained in terms of plasma pinching. Since in the presence of a molecular gas the plasma is shorter, the point of highest excitation is necessarily lowered. The plasma is more energetic in mixed gas plasma since the energy density has increased as a result of pinching.

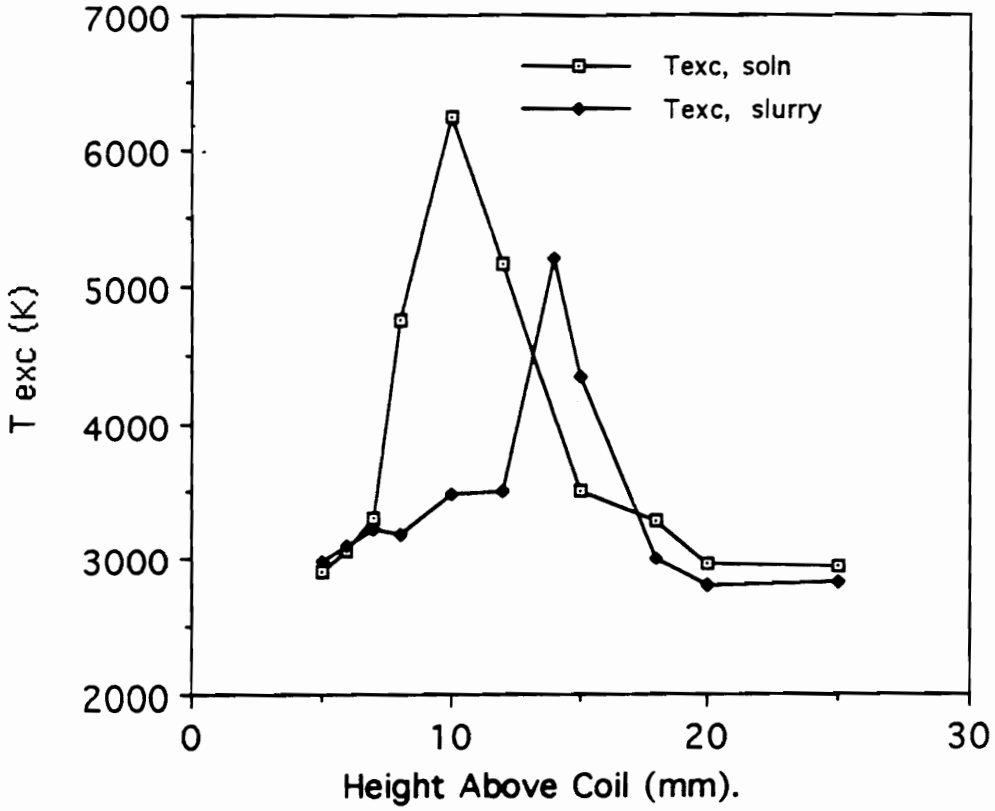

Figure 27. Excitation temperature profile for solution and slurry samples. Ar/Nitrogen (4%) Plasma.

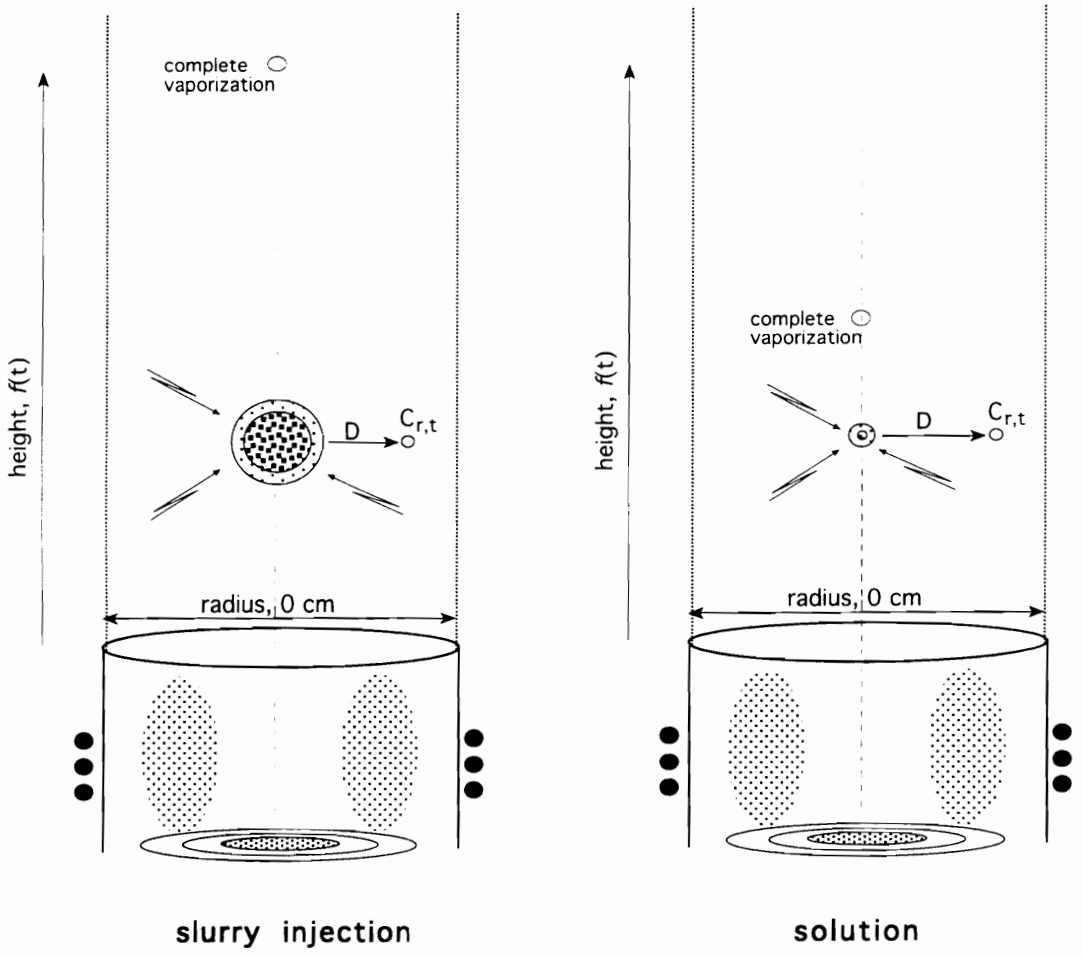

Figure 28. Comparison of vaporization rates between analyte in slurry and in solution.

Comparison of excitation temperature profiles indicates that the temperatures obtained from probes in slurry (Fe_2O_3) has its highest value higher up the plasma than the probes in solution (Fe^{2+}). This happens both in pure argon plasma and mixed gas plasma. For example, in pure argon plasma (Figure 26) the highest excitation temperature (solution) was 15 mm above the induction coil, whereas for slurry it was 18 mm. Similarly, in Ar/N_2 plasma (Figure 27), the measurements were 10 mm and 14 mm, respectively. Thus, there is a difference of 3-4 mm for maximum T_{exc} when a Fe_2O_3 slurry is used as a source of Fe atoms and when Fe^{2+}, the traditional source, is used for this purpose. Assuming the velocity of plasma gas to be about 10 m/s, this lag is about 0.3 millisecond.

Since excitation temperature of a plasma (or any such spectrometric source of energy) is obtained from measuring the population of excited levels of spectral lines, or more precisely, the ratio of upper level excited states to lower levels (including ground levels), as explained earlier in this chapter, the observed lag of highest excited levels from slurries points to the fact that there is some difference in the relative vaporization rates of atoms in slurry and in solution. One of the most puzzling questions in analytical spectrometry regarding mechanisms, is whether vaporization is heat-transfer controlled or mass-transfer controlled. The following discussion will attempt to explain the difference in slurry and solution excitation profiles in terms of vaporization mechanisms. The discussion should help provide some indication on whether the process is mass or heat transfer controlled.

Mechanism of Vaporization: A number of separate events occur sequentially in a flame or a plasma to convert a sample solution or slurry to free atoms. The most important of these are desolvation of the sample droplets and vaporization of the

resulting solute particles. Hieftje and associates have reported details of the desolvation [57, 58] and vaporization [59] processes. In these studies, the individual steps in the processes of desolvation and vaporization were demonstrated using an isolated droplet technique.

Desolvation: During desolvation, the solvent in a droplet of solution traveling through a flame/plasma is evaporated until one or more solid solute particles remain. The rate of desolvation is controlled by the conduction of heat from the surrounding flame/plasma gases to the surface of the droplet according to the equation [58].

$$D_o^2 - D^2 = k_1 t \tag{7}$$

where D_o is the initial droplet diameter, D is the droplet diameter at any time t after its entry into the flame/plasma and k_1 is the desolvation rate. Since this process is clearly heat-transfer controlled, the desolvation rate depends on the thermal conductivity of the gases surrounding the droplet and the source temperature.

Vaporization: This is the process in which a solid solute particle produced by desolvation is converted to species in the vapor phase. The mechanism for this process depends upon the nature of the solute, the source temperature, and the particle size. Relatively volatile solutes such as alkali metal salts are rapidly heated to their boiling point, after which vaporization of the material occurs. If the boiling point is appreciably lower than the source temperature, conduction of heat from the source gases to the surface of the molten particle will be the rate limiting process for vaporization. Thus, the process is described as **heat-transfer** controlled vaporization.

For high boiling point solutes, large solid particles, refractory salts and oxides, where the boiling point and the source temperature are not too different, **mass-transfer** could become the rate limiting mechanism [60]. Mass transfer controlled vaporization of a solid would be limited by the diffusion of gaseous solute away from the particle. The vaporization rate would then depend upon the diffusion coefficient of the solute vapor, the solute volatility and the source temperature. In this case Equation 1 that was used to describe desolvation rate, can still be used to describe vaporization rate k_1 [59, 60].

The fundamental difference between analytes in solution and in slurry is particle size. In this experiment, the mean diameter of the Fe(III) oxide used is reported by the vendor (Aldrich) as < 5 μm. On the other hand, the mean diameter of dry particles formed upon desolvation of droplets produced by concentric nebulizers of fairly dilute solution (below 1000 μg/mL), is in the order of less than 0.1 μm [59]. It was explained above that mass transfer controlled vaporization is limited by the diffusion of gaseous solute away from the particle; hence, the rate of vaporization depends on the diffusion coefficient of the solute vapor and the solute volatility. Certainly the larger particles of a slurry are less volatile than the smaller particles from solution. It is this difference in volatility between Fe from aqueous solution and Fe in Fe(III) oxide that results in the difference in the rate of vaporization. The lag in the appearance of highest T_{exc} for slurry compared to solution (Figure 26 and 27) is indicative this difference. The fact that this lag is observed in both argon and mixed gas plasmas in almost equal magnitude, indicates that the mechanism does not depend on the changes of thermal conductivity of the source gases (a condition for heat transfer), but mainly on the volatility of the solute. In other words, mass transfer rather heat transfer appears to be the vaporization rate limiting factor.

Mass Transfer: The profiles for slurries are shorter than solution profiles, *i.e.* less temperature is recorded using probes from slurries than from solutions. This apparent loss in temperature can be explained in terms of some energy being used in the process of sublimation. For some refractory material, atom production can depend also on the rate of sublimation of the heated solute [58]. Most of the energy is used to break down the large particles into smaller, more volatile particles before vaporization can take place.

An analyte particle in the plasma either from solution or slurry is surrounded by solvent vapor. The solvent vapor contains analyte in some concentration that is less than the concentration of analyte in the center of the particle. Due to this concentration gradient, *i.e.* high in the center of the particle and low away from the center, there is a movement of mass of solute from high to low concentration.

The mass-transfer mechanism can be mathematically modeled through the use of a diffusion equations based on Fick's laws [61]. The aim of this model operation is to express the rate of change of concentration of the particle as it evaporates in terms of the various parameters which govern this process, including the diffusion coefficient (volatility factor), number of molecules initially present (concentration) and the particle size. Let ϕ = the flux of matter in the particles, that is the rate of migration of material along the radius of the particle, in units of mol cm^{-1}, then

$$\phi = D\left\{\frac{\partial C(r,t)}{\partial r}\right\} \tag{8}$$

This is Fick's first law of diffusion, where D is the diffusion coefficient, C is the concentration of analyte, and r is the distance from the center of the particle, *i.e.* radius. For a spherical object, Fick's second law is

$$\frac{\partial C(r,t)}{\partial t} = D\left\{\frac{\partial^2 C(r,t)}{\partial r^2} + \frac{2}{r}\left(\frac{(\partial C(r,t)}{\partial r}\right)\right\} \tag{9}$$

By solving Equation 9 for $C_{(r,t)}$, the concentration of the diffused material at a given radius and time can be found. To solve this derivative equation, the Laplace transform is used and the following solution is obtained.

$$C(r,t) = \frac{C'}{2r(\pi Dt)^{1/2}} \int_0^a \left(\frac{r'\{e^{-(r-r')^2}}{4Dt - e^{-\frac{(r+r')}{4Dt}}} \right) dr' \tag{10}$$

where C' = initial concentration

r' = initial radius

a = initial volume

r = solved radius

If $N_t = C' \times 4/3\pi r^3$, then

$$C(r,t) = \frac{N_t}{8(\pi Dt)^{3/2}} \times e^{\frac{-r}{4Dt}} \left(1 + \left(\left(\frac{r^2}{Dt} - 6\right) \frac{a^2}{4Dt}\right)\right) \tag{11}$$

thus,

$$C(r,t) = \frac{N_t}{8(\pi Dt)^{3/2}} e^{\frac{-r}{4Dt}} \tag{12}$$

Equation 12 expresses the concentration of analyte in the particle at a given radius and time. This concentration depends on the number of moles, N_t, present to begin with, and the diffusion coefficient, D_t of the material in the analyte. Since the concentration of the analyte (Fe) was the same for solution and slurry samples used in this experiment (1000 ppm), and the diffusion coefficient must be the same for the same compound, Fe_2O_3, then the difference in $C(r,t)$ must be due to the difference in size of the particles.

Assuming that both particles from the solution and from the slurry undergo mass-transfer, i.e. diffusion process, the relative rate of diffusion will depend on the size of the particles. Thus the diffusion rate of analyte in slurry samples is less than that in solution samples. This explains the relative differences observed in excitation temperature measurements between the same thermometric species obtained from slurry and from solution. The difference in the diffusion rates is presented in Figure 28. In addition, due to the small particle size of analyte in solution, heat transfer might be more effective than mass transfer, a situation which would further enhance the rate of vaporization in solution contained analyte. Thus at a particular time t, that is at a height h, above the induction coil, less analyte will have evaporated into the plasma compared with the same parameters in solution.

Rotational Temperature: Rotational temperatures of the plasma were determined using the (O, O) band of the first negative system of the N_2^+ molecular ion when nitrogen was introduced in the plasma. On the other hand, the Q_1 band of the OH radical spectrum was used to obtain the rotational temperature when hydrogen was introduced into the plasma. The source of OH was water injected in the sample tube. The two emission bands are shown in Figures 29 and 230 respectively. For comparison purposes, the OH band was also used to determine the T_{rot} when nitrogen was

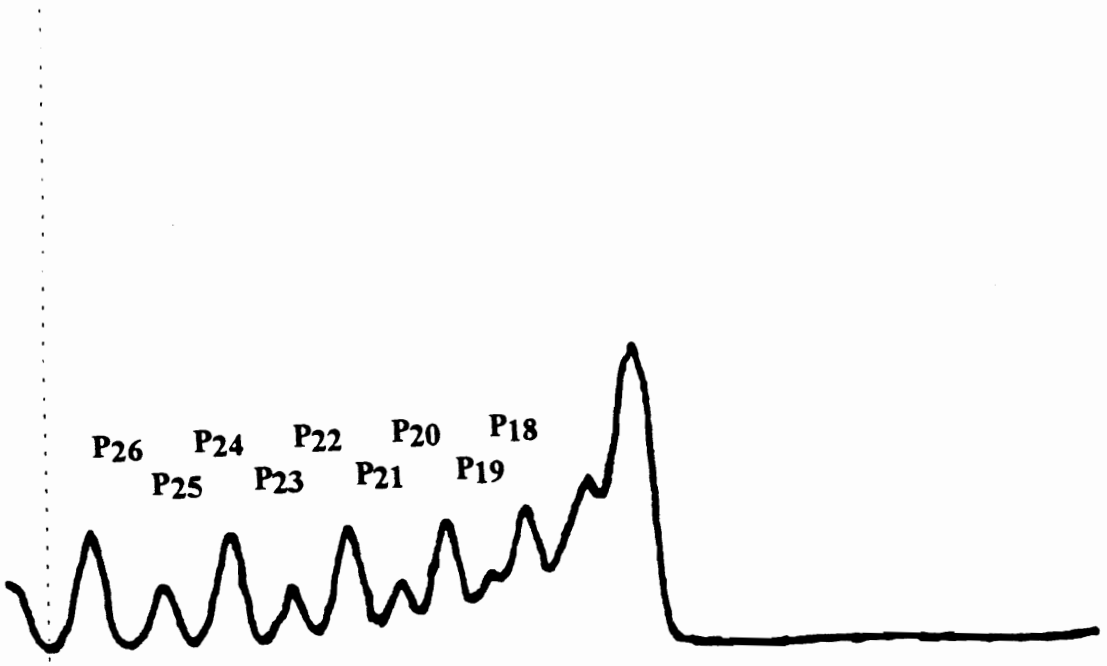

Figure 29. Rotational temperature measurements: N_2^+ emission band.

Table 9. Spectrometric constants of N_2^+ used in rotational temperature determinations: The P emission band

K	Wavelength (nm)	K (K - 1)
18	391.36	306
19	391.34	342
20	391.28	380
21	391.24	420
22	391.20	462
23	391.18	506
24	391.22	552
25	390.56	600
26	390.04	650

K = Quantum number.

introduced into the plasma. This information was important because the two thermometric species (N_2^+ and OH) could be compared under the same set of experimental conditions.

The N_2^+ system [$B^2 \Sigma u^+ - X^2 \Sigma g^+$ (O,O)] is in the 380.0 - 391.5 nm wavelength range. This system shows two spectral bands, called P and R branches. The spectra obtained in this work is mainly P branch between 391.4 and 391.0 nm, *i.e.* P_{18} to P_{26} according to reference [62]. Use of such a short spectral range is due to limited scanning width capability of the instrument which is only 1 nm. The scan was obtained between 391.0 and 392.0 nm.

From the experimental line intensity, I of the P branch, a straight line is obtained from the following relationship assuming a Boltzmann distribution between the rotational levels [55]:

$$\log\left(\frac{\alpha \times I}{K}\right) = f[K(K-1)] \qquad (13)$$

where α = 1 for even number lines and 2 for odd number lines, owing to the observation that the intensity of even lines is about twice the intensity of odd lines.

K = quantum numbers. In this case K ranges from 18 to 26

f = slope of the line = $2.983/ T_{rot}$

By plotting log [α x I/ K] versus [K (K - 1)], T_{rot} could be calculated from the slope. An example of the plot is given in Figure 31. In Table 9, the characteristic parameters of the P band are presented.

Using the Q_1 band of the OH radical spectrum, rotational temperature was obtained for hydrogen gas injection. The spectrum obtained ranged between Q_1 1 to Q_1 6 [63] and the band width was between 307.84 and 308.73 nm. The spectrum (Figure 30) was obtained while aspirating water, the source of OH. Table 10 gives the characteristic of Q_1 spectral band. The spectral assignment, energies and transition probability were made according to Dieke and Crosswhite [64].

The relationship used in this T_{rot} determination and derived by Boumans [53] is

$$\log I - \log A = -E_{exc} \times \left(\frac{\log e}{kT} \right) + \text{constant} \qquad (14)$$

where I = the intensity of the emission

A = rotational transitional probability

E_{exc} = excitation energy.

k = Boltzmann constant

T = transitional temperature.

By plotting [log I - log A] versus E_{exc}, a straight line with negative slope is obtained. The slope is equal to log e/kT. Rotational temperature is calculated from the slope.

Rotational temperatures were determined when the additional gas was introduced as cooling gas and also as injector gas in the range of 0.15 L/min to 1.5 L/min. Just like excitation temperature, data were obtained for both N_2 and H_2.

Figure 32 shows a comparison of the rotational temperatures obtained in the presence of nitrogen and hydrogen gas in the cooling gas stream. This figure indicates that, under the experimental conditions used, the maximum rotational temperature from both nitrogen and hydrogen mixed plasmas was obtained at about 4 -5% which is equivalent to 0.6 - 0.75 L/min of the cooling gas. The presence of nitrogen, however,

provides a higher temperature (about 8300 K) than hydrogen which was about 6000 K. In both cases the distribution of temperature measured was such that it was low for lower (< 4%) and higher (> 6 %) molecular gas content. This observation is very similar to that reported by Ebdon and Goodall [15], although in their experiments they introduced hydrogen in the injector gas.

In Figure 33, the rotational temperatures obtained in the presence of nitrogen and hydrogen in the injector gas stream are compared. The presence of about 15% *i.e.* 0.45 L/min hydrogen and 20 -25% (0.6-0.75 L/min) nitrogen appear to cause the highest rotational temperatures. Considering the error in this measurement which was 4%, the difference in these two maxima is not significant. It is important to notice at this point that just like emission data and unlike excitation temperature data, rotational temperature demonstrate, the self limiting effect of mixed gas plasma.

It should be noticed that there were two different thermometric species used in these experiments, *e.g.* N_2^+ and OH. The former was mainly used when nitrogen was injected, while the latter when hydrogen was injected. Thus it is difficult to draw rational conclusions on the effect of nitrogen and hydrogen based on data obtained using different probes. For this reason, an experiment was performed, in which OH emission band was used as the thermometric species when nitrogen is mixed with cooling gas and also injector gas. Results of such measurements are presented in Table 11. In this table, a summary is provided for all T_{rot} measurements.

Several observations are apparent from this table. (1) Generally, higher temperatures are obtained from mixing the molecular gases in the cooling gas stream than in the injector. This difference was explained earlier in this chapter as being a result of more thermal pinching associated with mixing in the coolant than there is in the injector. In the latter, the plasma axis becomes expanded, resulting in less plasma-analyte contact.

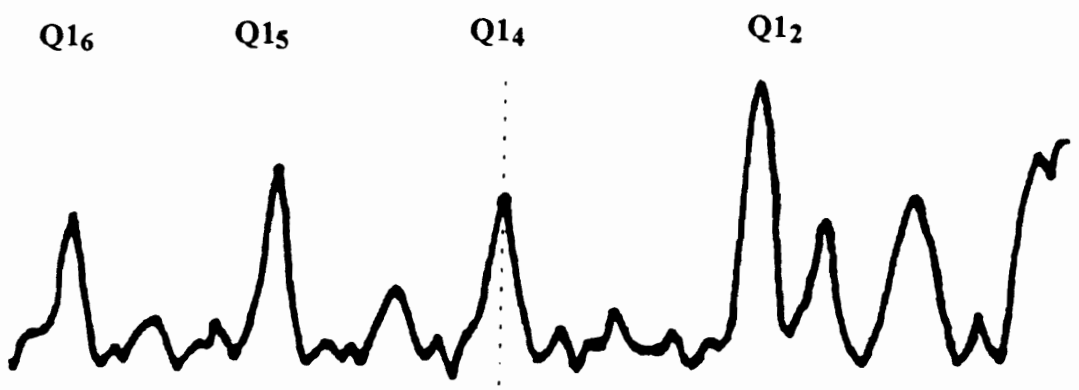

Figure 30. Rotational temperature measurements : OH emission band.

Table 10. Spectrometric constants of OH used in rotational temperature determinations: The Q_1 emission band

K	Wavelength (cm)	E_{exc} (cm)	A (10^8 s^{-1})
1	307.84	32475	10.0
2	307.99	32543	17.0
4	308.33	32779	33.7
5	308.52	32948	42.2
6	308.73	33150	50.6

E_{exc} = excitation energies.

A = Rotational transition probabilities.

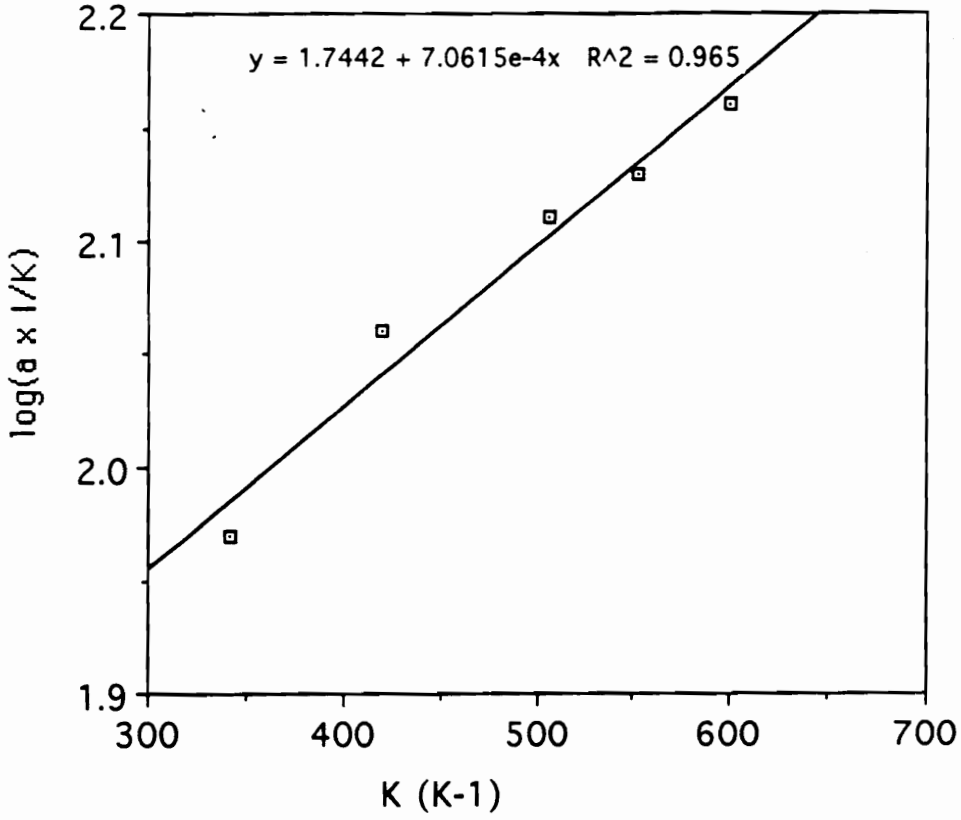

Figure 31. Boltzmann Plot: Rotational temperature measurement. Thermometric species N_2^+

The analyte in this case being the molecular gas. (2) It appears that the N_2^+ thermometer indicates higher temperatures than the OH thermometer. This observation was explained by Raeymaekers and associates [65] as due to the high dissociation rates of OH. For this reason, the population of the rotational levels may be considered as severely distorted so that temperature measurements yield doubtful results. (3) The temperature measurement precision in cooling mixed gas is generally better than in injector gas. This is partly due to the plasma instability often times noticed when introducing molecular gases in the injector, in which case the added gas has to pierce right in the center of the plasma discharge.

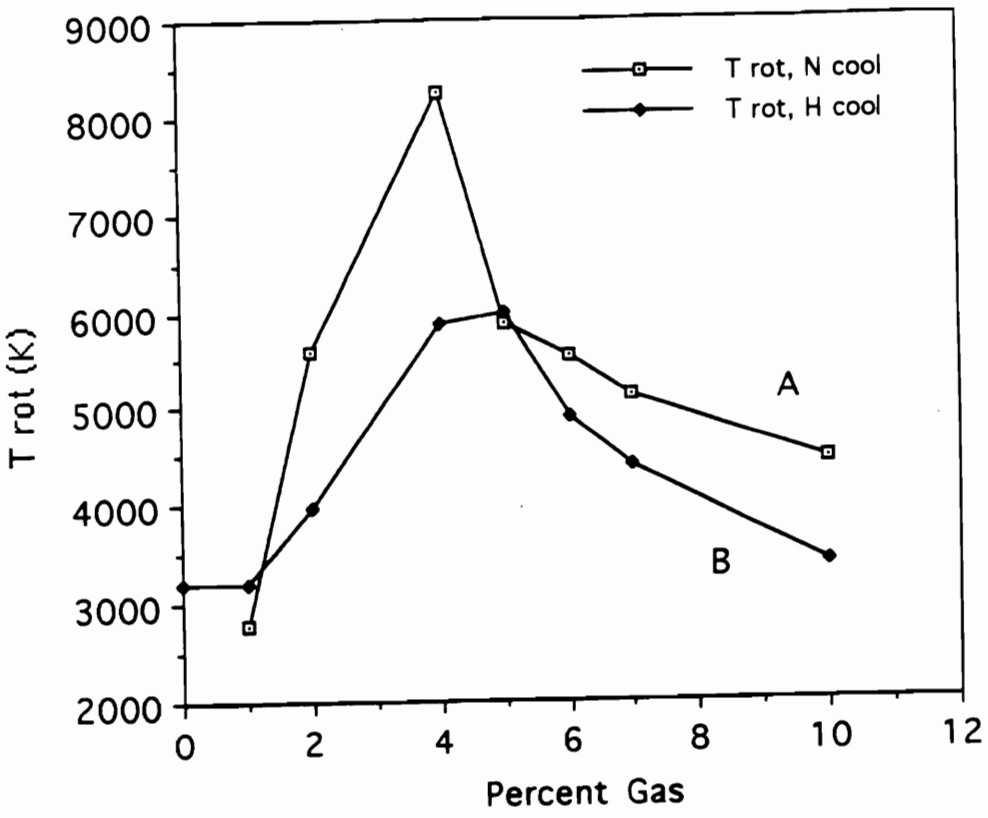

Figure 32. Comparison of T_{rot}: nitrogen and hydrogen in cooling gas. Thermometric species: A = N_2^+, B = OH

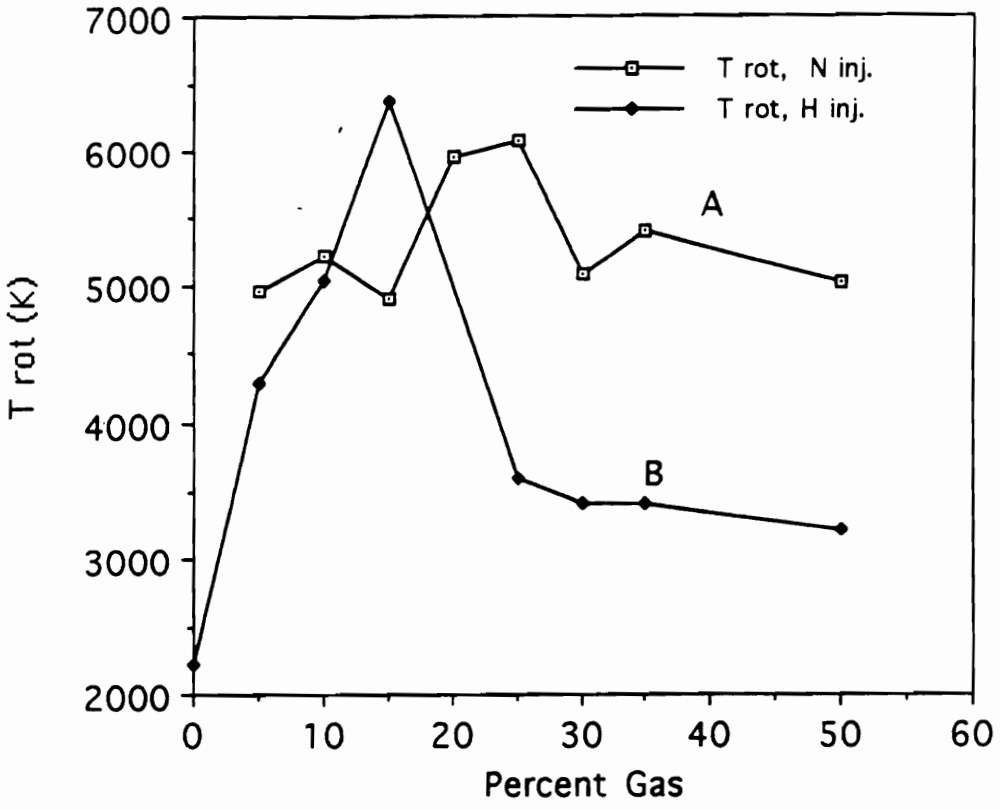

Figure 33. Comparison of T_{rot}: nitrogen and hydrogen in injector gas. Thermometric species: A = N_2, B = OH

Table 11. Rotational temperature measurements summary†

Plasma	**Thermometric species**	**Temperature* (K)**
Ar - N_2 cooling	N_2^+	8260 (150)
	OH	5850 (200)
Ar - N_2 injector	N_2^+	6080 (350)
	OH	4800 (150)
Ar - H_2 cooling	OH	5990 (200)‡
Ar - H_2 injector	OH	6380 (460)‡

* Error in parenthesis

† Temperature values are those measured when 0.6 L/min of hydrogen and/or nitrogen are mixed in the cooling and injector gas stream.

‡ Not statistically different

Summary: This chapter has characterized mixed gas plasmas in terms of the temperature obtained, as a function of nitrogen and hydrogen contents. The diagnostic studies show that more energy as well as better measurement precision are obtained when such gases are mixed in the cooling rather than the injector gas stream. This was the case for both excitation and rotational temperature measurements. Nitrogen rather hydrogen, generally provides higher temperatures to the plasma due to higher thermal conductivity of nitrogen compared to hydrogen.

Measurements of excitation temperature as a function of the molecular gases, have shown no self-limiting phenomenon of the mixed gas, indicated by rotational temperature and also emission intensity. This difference has been explained in terms of energy being lost, to "collisions of the second kind" such that not all plasma temperature is available to cause molecular vibrations or emitted as light quanta.

The difference in particle size for slurry and solution has been used in this study to derive the mechanism of analyte vaporization in the plasma. Mass transfer rather than a heat transfer mechanism seems to be the controlling factor.

The use of N_2^+ as the thermometric species in rotational temperature measurements is a better choice than OH radical. The latter has been reported by other researchers as having a higher dissociation rate and therefore tends to show lower and unreliable temperature values than the former.

Chapter 5

APPLICATION OF SLURRY INJECTION TECHNIQUE: DETERMINATION OF METALS IN SRMs

Introduction In the previous chapters the size dependent problems of analyte transport and analyte vaporization in slurry injection plasma emission spectrometry have been surmounted through the use of viscosity thickening agent in the analyte matrix and addition of N_2 to the cooling gas. Specifically, the use of PEO increases the nebulization efficiency of the Babington nebulizer and thus increases the mass of analyte that is transported to the plasma, while the addition of N_2 to the cooling gas increases the temperature of the plasma by about 20%, thereby promoting a higher degree of analyte vaporization.

This chapter demonstrates the applicability of slurry injection as a method of sample introduction into mixed gas inductively coupled plasma atomic spectrometry. Here a comparison of percent recovery of selected metals in standard reference materials is made between the traditional, U. S. Environmental Protection Agency recommended Method 200.2 and the slurry injection/mixed gas plasma method. The former method, known as "Hot-plate Extraction" involves digestion of solid samples including soils, sediments and urban particulates using a mixture of concentrated HCl and HNO_3. The digestion is performed on a hot plate at about 85^0 C for 30 minutes. It is assumed that within the extraction period, most water/acid soluble metals must be extracted. Following extraction, the sample (solution and solid) is centrifuged at about 2500 rpm for 20-30 minutes. After centrifugation some solid material containing undigested material, mostly silicates, remains. The solution is separated by decantation and injected into an argon ICP

through a concentric nebulizer. In the EPA project conducted in this study in 1991/92, known as "Hot plate Extraction Recovery Study" (HERS), percent recoveries were determined based on mass of metal contained in a unit mass of sample (μg/g). A complete description of this method is found in Appendix A. Results of the analysis using slurry injection or HERS on these SRM samples are subjected to statistical analysis. A comparison of these two methods serves as an appraisal to slurry injection technique which is a non-traditional, yet direct and potentially convenient determination of metals.

Selection of Metals that were Analyzed: The objective of this chapter was to determine the concentration of metals in trace levels using slurry injection and HERS in standard reference materials and evaluate the effect of particle size on the analysis. The SRMs evaluated were chosen primarily on the basis of particle size, and elemental composition. In order to avoid bias in the analysis from limited analyte sensitivity, only elements with certified values above the limits of quantification (LOQ) were considered.

Another important criteria used for metal selection was the sample particle size. Standard reference materials selected for analysis had to represent two groups: (1) those with small particles size (≤ 7) and (2) those with large particle size (≥ 10). This criteria was necessary because the effect of particle size, which is very important in slurry analysis could be demonstrated.

In reviewing the certificate of analysis and results of particle size analysis of the element Ca, Fe and Mg were present at trace levels in all the samples. Additionally one sample, NIST-1579 (Pb based paint) was selected for analysis because of its unique composition and small size.

Analytical Sensitivity: Prior to analyses of "real" samples, it was necessary to determine how the emission signal varies with the concentration (mass) of analyte. Plots of signal vs analyte concentration (working curves) were constructed for all elements using aqueous samples. Curves for HERS employed a pneumatic nebulizer and Ar discharge. Curves for slurry injection used the Babington nebulizer, PEO, and a mixed gas plasma. For each plot the slope of the line (analytical sensitivity) was determined. Also LOQ and the limit of linearity (LOL) was determined. All analysis were performed in the concentration range between the LOQ and LOL. Also from such a plot, information concerning the convenient amount of material to be analyzed can be obtained. Such curve is shown in Figure 34.

Effect of Particle Size: Particle size is of fundamental importance in the quantitative analysis of samples by slurry injection ICP-AES. Previous studies report that slurries having a particle size of greater than 1.5 μm cannot be successfully analyzed by this method [20]. Ebdon *et al.* [66] concluded that the bulk of the particles should be less than 3 μm for slurries to show comparable mass transfer efficiencies with solutions. However, it has also been reported [67] that, sample transport could be improved by using a "straight through" spray chamber, like the horn-shaped type used in this study. This minimizes impaction losses common in Scott-type, double or single barrel spray chambers. Thus, large particles which would otherwise have adhered to the sides of the impaction surfaces and drained away, can reach the plasma. With such a spray chamber, kaolin particles up to 8 μm could be successfully analyzed for Fe, Mg, Ti and Si. in the ICP [67].

The selection of SRMs to be analyzed required knowledge of mean particle size, in order to assess the likelihood of efficient analyte transport and vaporization. Smaller

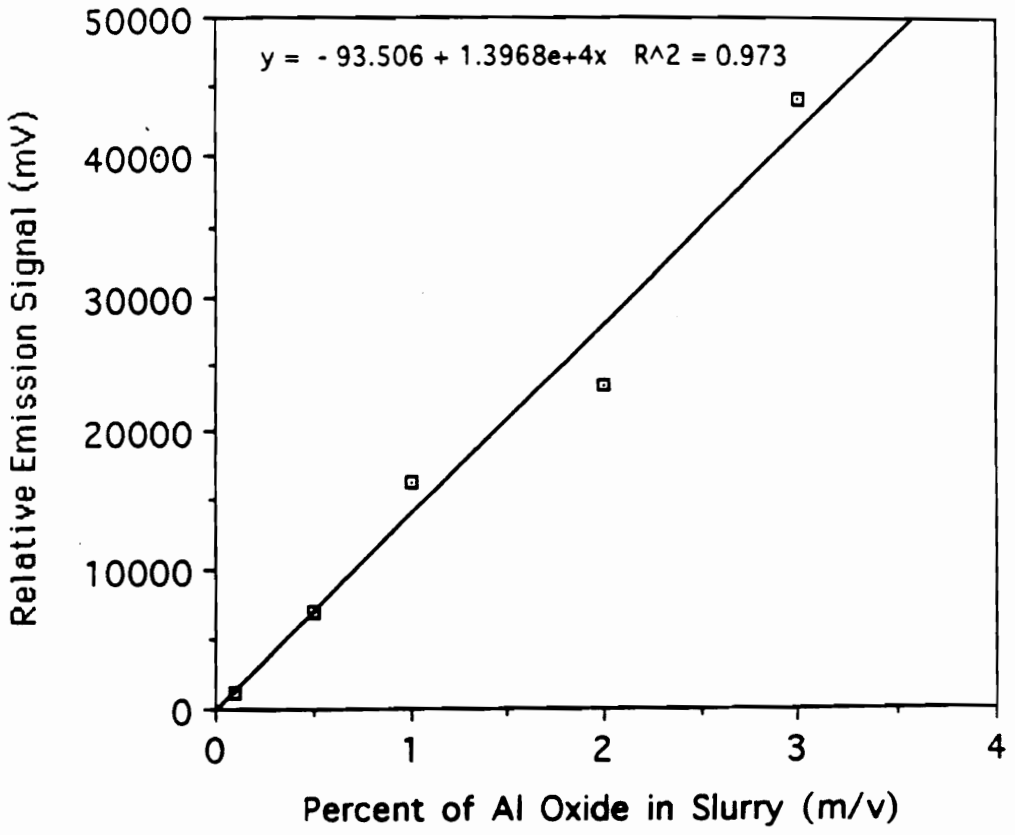

Figure 34. Sensitivity of the method. Relationship between mass of analyte and emission signal.

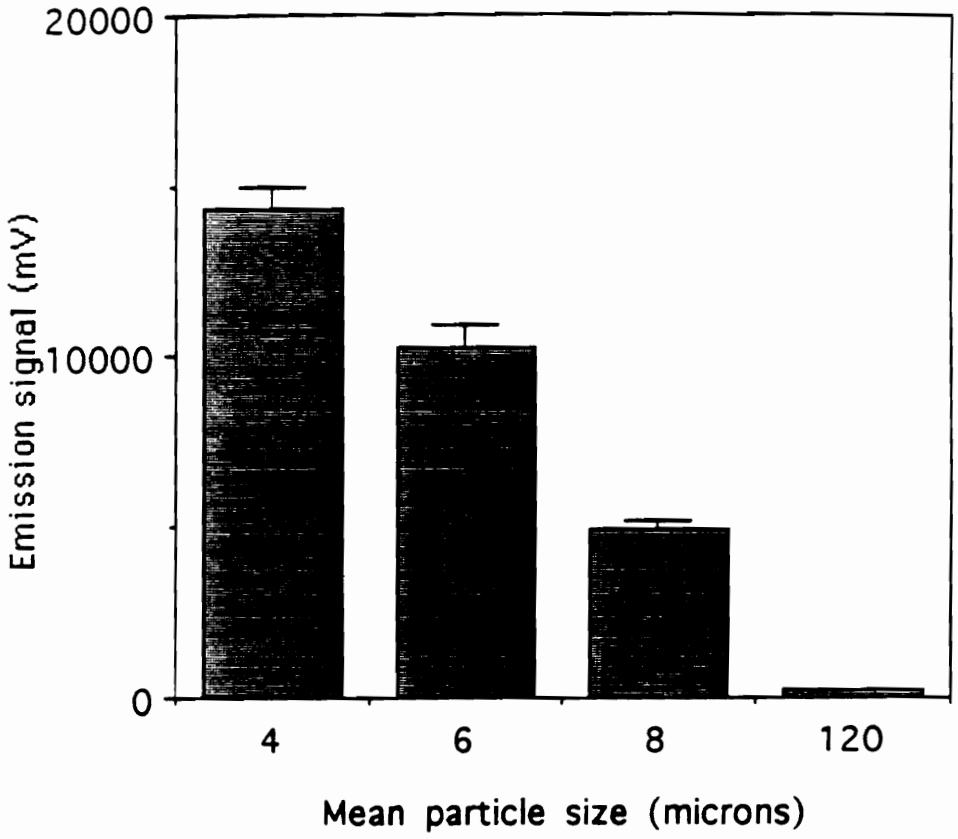

Figure 35. Effect of particle size on emission signal (Al 396.15 nm). All slurries were 1% (m/v). Size 120 corresponds to unground sample.

particles are easily transported and vaporized in the plasma compared to larger particles. This fact is confirmed by analyzing equimolar samples with different particle sizes of alumina for aluminum atomic line at 396.152 nm and comparing the emission signals. As seen in Figure 35, particles with 4 μm mean diameter provide much higher signal than 6 μm, 8 μm and 120 μm. The relative grinding time of the bulk alumina to achieve these sizes was respectively 30, 15, 5 and 0 minutes. It should be noticed that, the latter size corresponds to the mean diameter of unground alumina.

With this information on signal and sample size, 10 SRM samples were evaluated for mean particle size. Out of these, 3 were found to between 4 and 7 μm. The rest ranged between 40 and 60 μm. Grinding of the samples was not considered because it would invalidate the certified values of Ca, Fe, and Mg.

Data Collection Procedure: 1. EPA Method 200.2: The hot-plate extraction was performed as explained in the previous section. Prior to determining the metal concentration in the unknown samples, calibration curves were constructed for each metal. Standard solutions were made from stock solutions (Spex-Plasma Standards) containing 1000 μg/mL in 5% nitric acid matrix. Distilled deionized water was used to make serial dilutions. The calibration curves were linear. Sample introduction for both standards and unknowns was accomplished by the use of a standard pneumatic, Meinhard nebulizer. The plasma used in this analysis was a pure argon plasma as stipulated in the EPA 200.2. The total concentration of the metal in the unknown sample was then calculated in terms of μg/g of sample based upon the sample weight used and the volume of the solution.

2. Slurry Injection Method: Slurries were prepared as described in Chapter 2. A calibration curve was constructed for each metal, using aqueous solutions in which appropriate concentration of PEO was added. For both standards and slurries, sample introduction was facilitated by the use of the Babington nebulizer. The plasma in this case was a mixed gas type, comprising of 4% Nitrogen and 96% Argon. Based on results in Chapter 3 and 4, the molecular gas was added as part of the cooling gas. The observation point was set at 10 mm above the coil and the flow rate used was 1.0 mL/minute. The total concentration of the metals in the unknown sample was calculated in terms of μg/g of the sample based on the sample weight and volume of slurry, which was invariably 100 mL.

Comparison of the Two Methods: Comparison of the two sample introduction methods, that is slurry injection and EPA 200.2 (HERS), in which solutions are introduced, was accomplished by comparing the percent recovery of the metals of interest for the two methods. In this context, percent recovery is defined as follows:

$$\% \text{ Recovery} = \frac{\text{Found conc. of metal in the SRM (μg/g)}}{\text{Certified conc. of metal in the SRM (μg/g)}}$$

The certified concentration was provided by the NIST or the other reference material authority as listed in Table 3. For the purpose of this comparison, the certified concentration was regarded as 100% concentration. The "found" concentration is the amount determined by either of the two methods.

Table 12 compares the two methods in terms of percent recovery of Ca, Fe, Mg in four samples and Pb in one sample. The Table shows two groups of samples. In one group the two recoveries are statistically significantly different and in another they are

not significantly different. These differences were evaluated through the use of 2-tail student t-test. Through this statistical tool, it was demonstrated that, for sample BCR-176, which has mean diameter 4.5 μm, the recovery of Ca, Fe and Mg was not statistically significantly different when the slurry injection method or the EPA-200.2 method were used. Also for sample BCSS-1, the recovery of Ca showed no difference in the two methods. All other measurements were rejected as being statistically significantly different at the 95% confidence level. In all cases, however, the precision in the determinations using slurry injection was not statistically different from the EPA 200-2 method at a 95% confidence level according to F-test.

It is important to mention that although the percent recovery of Pb in NIST-1579 was significantly less in slurry injection method than it was in the EPA 200.2 method, the recovery of the new method was impressively high (81%). This was so despite the large particle size (7.6 μm) of this sample.

Table 12. Percent recovery of selected metals: Slurry injection with mixed gas plasma *versus* solution injection with Argon plasma

		Percent Recovery		
Sample	**Element**	**Slurry injection*.**	**EPA-200.2.***	**Size (μm)**
NIST-1575	Calcium	57.6 (4.5)	100.3 (4.0)	45.4
	Iron	21.0 (3.7)	53.9 (13.7)	
	Magnesium	ND	ND	
BCR-146	Calcium	38.6 (2.9)	77.5 (5.7)	59.3
	Iron	23.5 (3.5)	62.3 (6.9)	
	Magnesium	27.4 (3.0)	58.3 (1.8)	
BCSS-1	Calcium	47.7 (8.4)‡	54.1 (12.3)‡	4 .5
	Iron	47.8 (3.2)	89.5 (14.8)	
	Magnesium	42.2 (5.2)	59.2 (4.1)	
BCR-176	Calcium	76.0 (2.8)‡	79.8 (0.7)‡	4 .5
	Iron	62.1 (4.5)‡	61.8 (16.6)‡	
	Magnesium	39.5 (2.9)‡	41.0 (1.4)‡	
NIST-1579	Lead	80.8 (2.9)	97.3 (2.1)	7.6

* Errors in parenthesis. All errors are one standard deviation from the mean.

‡ Recovery pairs not significantly statistically different

The particle sizes represent mean diameters.

Summary: The direct determination of metals using slurry nebulization of environmental samples has been compared to the conventional EPA method of solution nebulization. The slurry injection method shows adequate analytical sensitivity. The precision of slurry injection, that is, the uncertainty of the measurements was comparable to the error obtained from solution injection method. Where the mean sample particle size was as small as about 5 μm in diameter, the recovery did not statistically differ from that of the EPA method. This similarity in recovery shows that the efficiency of analysis of the new method could be as good as the established method. There is some indication that the method is potentially capable of analyzing samples with even greater diameters, as evidenced by the high percent recovery of Pb in a sample with 7.6 μm. It should be noted that both methods show bias in the recovery with increasing sample size and sample morphology. BCR-146 had a 77.5% recovery by HERS. It is a municipal sludge and primarily a mixture of inorganic and organic material. The NIST-1575 is a standard reference material of pine needles, hence an organic material. The large size of BCR sample coupled with potentially refractory composition could retard extraction by HERS and slurry injection.

The improved analytical performance of the slurry injection technique was possible because of the modifications made in both the sample introduction and the plasma discharge. These modifications included the use of clog-free Babington nebulizer, thickening agent/surfactant, and mixed gas plasma. The type of spray chamber used was also very appropriate for slurry injection. The results reported in this study, that is, the possibility of analyzing slurries having particle size as large as 5 μm with similar efficiency as solutions, are much better than reported in prior studies (20,66). In those previous studies, it was suggested that, to achieve similar analysis efficiency from slurry and solution introduction, the cut-off point of slurry particle size, is 1.5 μm.

Chapter 6

CONCLUSIONS

The primary goal of this research project was to evaluate slurry sample injection, an alternative method of sample introduction into an ICP, and the use of mixed gas plasma as a more energetic vaporization medium than a pure argon plasma. Small amounts of a surfactant, polyethylene oxide were added to the slurry to enhance the sample introduction capability of the Babington nebulizer. At medium sample flow rate (1 mL/minute), it was found that the presence of about 5 ppm (μg/mL) PEO increased the emission signal of elements in slurry matrix to approximately 45%. Further enhancement in the signal was obtained with the addition of small amounts of nitrogen gas into the cooling gas stream. Plasma containing about 4 -5% nitrogen showed optimum enhancement.

Whereas prior studies concluded that some surfactants provide enhancement of signal due to improved transportation resulting from reduced droplet size of the aerosol as a consequence of reduced surface tension, PEO seems to provide efficient nebulization due to slightly elevated viscosity. The viscosity effect of PEO in the slurry was found to be more important than the surface tension in determining the size of droplets. The Nukiyama-Tanasawa relationship was used to predict the droplet size of the aerosol produced at various concentrations of PEO.

Two modes of introducing molecular gas into the ICP were explored; (1) as part of the cooling gas also known as outer or plasma gas, and (2) as part of the injector gas. The latter is also known as the nebulizer or inner gas. Application of nitrogen and hydrogen was compared in terms of plasma temperatures, which is the source of energy necessary

for atomic excitation. This study has found that, the outer mixed gas provides higher temperatures than the nebulizer mixed gas fashion. The signal enhancement effect of mixed gas is described as a direct consequence of higher thermal conductivity of molecular gases compared with mono-atomic argon. Due to higher thermal conductivity of nitrogen and hydrogen, the plasma becomes more energetic than pure argon plasma.

Measurements of excitation and rotational temperatures confirm that mixed gas plasmas are more energetic than pure argon plasmas. Associated with the higher temperature was thermal pinch, a reduction of plasma size. In this study it was found that the volume of the plasma decreased significantly with increasing concentration of molecular gas. As expected, nitrogen containing plasma provided higher temperatures than hydrogen containing plasma. This difference is expected because the thermal conductivity of nitrogen is about 14 times that of hydrogen.

The effect of mixed gases is self-limiting; that is the emission intensity increases up to some concentration of the molecular gas and decreases with further increments of the gas concentration. This self-limiting effect was also demonstrated in rotational temperature data. However, excitation temperature versus amount of molecular gas plots do not show this phenomenon. This deviation is rationalized as being due to the fact that, since T_{exc} is a measure of the ratio of excited, upper level species in the plasma (atoms, ions, molecules, etc.) to lower levels, the ratio will increase as long as the thermal conductivity increases. But since less emission signal is obtained despite high T_{exc} above 4% nitrogen, an event must be occurring in the discharge that reduces the available energy. This loss of energy has been described by Boumans in terms of "collision of the second kind" whereby, excited states are destroyed on collision without emitting radiation in the form of light quanta.

The use of Fe(III) oxide slurry as a source of Fe (the thermometric species) in the determination of T_{exc} and its comparison with $Fe^{2+}_{(aq)}$ source has aided in the correct prediction of vaporization mechanism. Data from temperature/height above coil profiles of the two approaches and application of Fick's laws of diffusion suggest that slurry vaporization is most likely mass transfer controlled rather than heat transfer controlled. In the mass transfer mechanism, matter diffuses from high to lower concentration, that is from the center of the particle to the periphery. The rate of diffusion depends among other factors on the particle size of the sample analyte. On the other hand, in the heat transfer mechanism, heat is absorbed from the plasma into the analyte particle. Expectedly, the effectiveness of the heat transfer mechanism depends on the temperature of the plasma gases surrounding the analyte.

Evidence to support this conclusion was provided by the observation that slurry particles spent more time in the plasma (traveled longer) than in solution before the highest excitation temperature was recorded. Vaporization and ultimately excitation of analytes in the slurry matrix showed a tendency to lag behind analytes in solution. If heat transfer were the controlling factor in the production of vapor phase analyte atoms, then, mixed gas plasma, eliminate or at least reduce this lag because of the availability of higher energy. In other words, if the surrounding temperature is high (high thermal conductivity), vaporization should take place faster than in the normal plasma. Thus, even large particles in slurries would be dissociated and evaporated as fast as solution contained analyte. The similarity of T_{exc} profiles in pure argon and mixed gas plasma is strong evidence of a mass transfer controlled vaporization mechanism.

Analyses of real environmental samples (Standard Reference Materials) showed that through this technique of modified sample injection coupled with modified plasma environment, the percent recovery improves dramatically provided the mean particle

diameter is not greater than 5 μm. The precision of the slurry injection technique compares favorably to hot acid extraction, for all samples, while the accuracy falls for slurry injection at highest particle diameters. However, the successful recovery of particles 5 μm is 3 times larger than particles injected into pure Ar plasma without surfactants.

The work that is presented in this dissertation provides some evidence that a non-traditional sample introduction technique in inductively coupled plasma, slurry injection, can be a potentially reliable method. Apart from somewhat higher relative error in accuracy involving slurry injection into mixed gas plasma compared to the traditional method, the former could be a method of choice especially when lengthy sample preparation procedures need to be avoided.

REFERENCES

1. G. D. Christian and J. E. O'Reilly, eds., "Instumental Analysis" 2nd edition, Allyn and Bacon, Inc., Newton Massachusetts (1986)
2. A. T. Zander, *Anal. Chem.* **58**, 1142 A (1986).
3. G. A. Meyer, *Anal.Chem.* **59**, 1345A (1987).
4. S. Greenfield, I. L. Jones, and C. T. Berry, *Analyst*, **89**, 713 (1964).
5. E. A. Stubley and G. Horlick, *Appl. Spectrosc.* **38**, 162 (1984).
6. P. Schramel and X. Li-Qiang, *Fresenius Z. Anal. Chem.* **319**, 229 (1984).
7. E. H. Choot and G. Horlick, *Spectrochim. Acta.* **41B**, 907 (1986).
8. E. H. Choot and G. Horlick, *Spectrochim. Acta.* **41B**, 925 (1986).
9. E. H. Choot and G. Horlick, *Spectrochim. Acta.* **41B**, 935 (1986).
10. B. S. Sheppard, W. L. Shen, T.M. Davidson and J.A. Caruso, *J. of Analyt. At. Spectrom.* **5**, 697 (1990).
11. S. Chan and A. Montaser, *Spectrochim. Acta.* **40B**, 1467 (1985).
12. A. Montaser and D.W. Golightly, eds., " Inductively Coupled Plasmas in Analytical Atomic Spectrometry", 2nd edition, VCH Publishers, Inc., New York (1992).
13. A. Montaser and R. L. Van Horen, CRC *Crit. Rev. Anal. Chem.* **18**, 45 (1987).
14. M. Capitelli, F. Cramosa, L. Triolo and E. Molinari, *Combust. Flame,* **15**, 23 (1970).
15. L. Ebdon and P. Goodall, *J. of Analyt. At. Spectrom.* **7**, 1111 (1992).
16. J. W. H. lam and G. Horlick, *Spectrochim. Acta.* **45B**, 1313 (1990).
17. A. Montaser, V.A. Fassel and J. Zalewski, *Appl. Spectrosc.* **35**, 292 (1981).
18. G. R. Kornblum and L. deGalan, *Spectrochim Acta* **32B,** 71 (1977).
19. J. A. Broekaert, W. A. Born, R. Klockenkamper, P. Tschöpel, and F.C. Adams, *Spectrochim Acta* **46B**, 1033 (1991).
20. I. B. Brenner, L. Halicz and O. Yoffe, *J. of Analyt. At. Spectrom.* **8,** 475 (1993).

21. L. Ebdon, P. Goodall and M.E. Foulkes *Spectrochim. Acta.* **48B**, 1563 (1993).

22. R. F. Browner and A.W. Boorn, *Anal. Chem.* **56**, 787 (1984).

23. S. W. McGeorge and E. D. Salin, *Appl. Spectrosc.* **39**, 989 (1985).

24. L. Ebdon and M. R. Cave, *Analyst*, **107**, 172 (1982).

25. S. Dresner, *Popular Science*, **May**, 102 (1973).

26. M. Wu and G. M. Hieftje, *Appl. Spectrosc.* **46,** 1912 (1992).

27. P. W. J. M. Boumans, ed. " Inductively Coupled Plasma Emission Spectroscopy". Part II. John Wiley and Sons, New York, 244 (1987).

28. A. G. T. Gustavsson, *Anal. Chem.* **55**, 94 (1983).

29. R. F. Browner, A.W. Boorn and D. D. Smith, *Anal. Chem.* **54**, 1411 (1982).

30. A. Canals, J. Wagner, R. F. Browner and V. Hernandis, *Spectrochim Acta*, **43B**, 1321 (1988).

31. M. Kodama and S. Miyazawa, *Anal. Chem.* **52**, 2358 (1980).

32. J. Farino and R. F. Browner, *Anal. Chem.* **56**, 2709 (1984).

33. J. Mora, V. Hernandis, and A. Canals, *J. of Analyt. At. Spectrom.* **6**, 573 (1991).

34. A. Ruiz, A. Canals, V. Hernandis, *J. of Analyt. At. Spectrom.* **8**, 109 (1993).

35. E. Pungor and M. Mahr, *Talanta*, **10**, 537 (1963).

36 J. Mora, A. Canals, and V. Hernandis, *J. of Analyt. At. Spectrom.* **6**, 139 (1991).

37. Z. Y. Yan and W. Zhang, *J. of Analyt. At. Spectrom.* **4**, 797 (1989).

38. T. McCreary, Ph.D. Dissertation, Virginia Tech (1988).

39. Instructional Manual for ICP/6000, Perkin Elmer, 1984, Norwalk, CT.

40. F. Daniels, R. A. Alberty, J. W. Williams, C. D. Cornwell, P. Bender and J. E. Harriman" Experimental Physical Chemistry" 7th edition. McGraw-Hill Book Co. (1970).

41. Instructional Manual for DCA-322, Kahn Instruments, Inc., Carritos, CA.

42. F. R. Meeks, J. S. Caruso, B. A. Bielski and I. Marawi, *J. of Analyt. At. Spectrom.* **7,** 899 (1992).

43. S. Nukiyama and Y. Tanasawa, *Trans. Soc. Mech.* (Japan), **4**, 86 (1938).

44. D. Meyers, Surfactant Science and Technology, 2nd ed. VCH Publishers, Inc. (1992).

45. A. W. Adamson, " Physical Chemistry of Surfaces" 4th edition, John Willy and Sons, NewYork (1982).

46. G. M. Barrow, " Physical Chemistry " 4th edition, McGraw - Hill, New York (1979).

47. A. Canals, J. Wagner, R. F. Browner and V. Hernandis, *Spectrochim Acta* **45B**, 591 (1990).

48. J. R. Welty, C. E. Wicks and R. E. Wilson, "Fundamentals of Momentum, Heat, and Mass Transfer," 3rd edition. John Wiley and Sons (1984).

49. I. B. Brenner and A. Verbeck , *J. of Analyt. At. Spectrom.* **4**, 23 (1989).

50. L. S. Gervais and E. Salin, *J. of Analyt. At. Spectrom.* **6**, 41 (1991).

51. D. J. Kalnicky, V. A. Fassel and R. N. Knisely, *Appl. Spectrosc.* **31**, 137 (1977).

52. W. L. Wiese and G. A. Martin, "Wavelengths and Transition Probabilities for Atoms and Atomic Spectrometry," Part II, NSRDS-NBS 68, Washington, DC (1980).

53. P. W. J. M. Boumans, " Theory of Spectrochemical Excitation", Plenum Press, New York (1966).

54. J. S. Bolton , " The Effects of Organic Gases on Atomic Spectrometric Signals in the ICP", Ph.D. Dissertation, Virginia Tech, Blacksburg, VA (1988).

55. M. H. Abdallah and J. M. Mermet, *J. Quant. Spectrosc. Radiat. Transfer*, **19**, 83 (1978).

56. S. J. Northway, R. M. Brown, R. C. Fry, *Appl. Spectrosc.* **34**, 338 (1980).

57. G. M. Hieftje, H. V. Malmstadt, *Anal. Chem.* **40**, 1860 (1968).

58. N. C. Clampitt and G. M. Hieftje, *Anal. Chem.* **44**, 1211 (1972).

59. G. J. Bastiaans and G. M. Hieftje, *Anal. Chem.* **46**, 901 (1974).

60. P. D. Johnston, *Combust. Flame*. **18**, 373 (1973).

61. G. L. Long and C. B. Boss, *Anal. Chem.* **54**, 2497 (1982).

62. M. H. Abdallah and J. M. Mermet, *Spectrochim. Acta*, **37B**, 391 (1982).

63. J. Cotrino, M. Saez, M. C. Quintero, A. Menendez, E. Sanchez Uria, and A. Sanz Medel, *Spectrochim. Acta*. **47B**, 425 (1992).

64. G. H. Dieke and H. M. Crosswhite, *J. Quant. Spectrosc. Radiant. Transfer*. **2**, 97 (1962).

65. B. Raeymaekers, J. A. C. Broekaert and F. Leis, *Spectrochim. Acta*, **43B**, 941 (1988).

66. L. Ebdon and M. E. Foulkes and S. Hill, *J. of Analyt. At. Spectrom.* **5**, 67 (1990).

67. L. Ebdon and A. R. Collier, Spectrochim. Acta. **43B**, 355 (1988).

APPENDIX A

HOT-PLATE METAL EXTRACTION PROCEDURE: US EPA METHOD 200.2

(Source: US EPA Atmospheric Research and Exposure Assessment Laboratory - Research Triangle Park, NC)

All sample containers must be cleaned with detergent, soaked for at least 4 hours in 20% v/v HNO_3, rinsed three times with ASTM Type I water and oven dried. Both linear polyethylene and Class A borosilicate glass containers are suitable.

Apparatus Hot plate or equivalent - capable of reaching and maintaining a temperature of 95^0 C, all the necessary glassware, centrifuge, 2500 RPM capability. Analytical balance capable of accurately measuring weights to the nearest 0.001 g. Polypropylene centrifuge tubes with screw tops of polypropylene, 50 mL volume (Nalgene 3119-0050).

Reagents Nitric acid (concentrated) - Redistilled spectrographic grade. Hydrochloric acid (concentrated) - Reagent grade.

Procedure Make 1 + 1 HNO_3 by adding 100 mL conc. HNO_3 to 100 mL ASTM Type 1 water. Make 1 + 4 HCl by adding 50 mL of conc. to 200 mL ASTM water. Place an accurately weighed portion of sample (about 0.5 g) in a 250 mL beaker. Add 4 mL of 1 + 1 HNO_3 and 10 mL of 1 + 1 HCl. Cover with a watch glass. Place on a hotplate. When all samples are in place put an open beaker containing 50 mL of water near the center of the of the array on the hot plate. Bring the water to approximately 85^0C. Maintain but do not exceed 85^0 C for 30 minutes. Transfer with rinsing into a 100 mL volumetric flask and make to volume with ASTM Type 1 water.

NB. The goal is to have a final matrix with about 2 and 5 mL, respectively, of the mixed acids per 50 mL of solution. Larger quantities could be used if a larger sample size were needed or difficulties are experienced in control of heating.

Pour into a centrifuge tube and centrifuge at 2500 RPM for 10 minutes.

Analysis All analyses of elements by ICP-AES must be completed in 72 hours after extraction. Prior to accepting data, establish that plasma overload of nonanalytes is unimportant by diluting the extract 1:10 or 1:25 with the final acid matrix.

APPENDIX B

DETERMINING INTERELEMENT CORRECTION FACTORS FOR ICP-AES

(Source: Same as Appendix A)

1. Prepare single element standards of the elements of interest.
2. Calibrate instrument with one element at a time.
3. Analyze that standard as a "sample" and use the "found" concentration for the calculations below.
4. Prepare 2 or more concentration levels of the potentially interfering element. These solutions must be single element solutions also. If the concentration levels typically encountered in the samples are known, make the top standard above these.
5. Analyze the interfering solutions from step 4 as "samples", acquiring data on all elements standardized in step 2 as well as on the interfering element. Use the "found" concentration, not the prep. value. [You get the most accurate data if you analyze the element of interest back-to-back with the potentially interfering elements]

   6. Calculations for Element of Interest: Determine the recovery of the single element standard for the element of interest to determine if the instrument was operating properly.

Interference correction factors

(a) Easiest for hand calculations or if only one concentration of the interfering element is used:

Correction factor = "apparent" Be conc found/V interference conc found

$$= \frac{ng"Be"}{ngV}$$

Then,

Corr. Be conc. = (Found Be conc) - (correction factor) (Found V conc)

Note: In this example, Be has been "background " corrected separately at the intensity level before the concentration is calculated from the calibration curve.

(b) For best corrections:

If two or more concentrations of the interfering element are used, plot the data to check linearity. If linear, fit with 1st order equation. If "apparent" concentration is not dependent on the interfering element's concentration, the "apparent" concentration is probably due to background or another interferent.

Use concentrations from the standards that were calculated as if the standard was a "sample" ("found" conc) to generate a table.

Example: Interference of V 310.230 on Be 313.042

	ng/mL	
Prep V conc	Found V conc	"Apparent Be conc"
0.000	5.1420	0.4628
1250	1185.0	8.6950
2500	2313.0	16.640
5000	4643.0	33.210
10000	9295.0	66.320

Then;

Corr. conc = (Be Found conc) - (0.00709) (V Found conc) - (0.31314)

All "samples" concentration are in net µg/mL or ng/mL, after background correction has been made.

You normally only have to go through the interference determination step once as it seems to be instrument (and its parameters) dependent, not sample matrix dependent. However, it is always good to check a new matrix's recoveries with a known, as subtle changes to the instrument's parameters may have occurred, *i.e* nebulizer performance, hazing of grating or optics, PMT settings, *etc.*

VITA

Ward J. Mavura

	A citizen of Tanzania, East Africa.
Undergraduate Education	Bachelor of Science, Chemistry, 1982 University of Dar es Salaam, Tanzania
Experience	Chemistry instructor, Dar es Salaam Teachers Training College (1982-1985)
Graduate Education	1. Master of Education, May 1987 University of Massachusetts at Amherst. 2. Master of Science, Chemistry, December 1990 Hampton University, Virginia. 3. Doctor of Philosophy, Chemistry, August 1994 Virginia Polytechnic Institute and State Univesity, Blacksburg, Virginia.
Dissertation	Determination of Metals using Slurry Injection in Inductively Coupled Plasma Emission Spectrometry Advisor: Dr. G. L. Long
Professional Societies	American Chemical Society Society for Applied Spectroscopy
Awards	The Chemistry Department Teaching Excellence Award, as an instructor in Instrumental Analysis. 1993
Present Employer	Slippery Rock University, PA Assistant Professor of Chemistry

Publications

I. T. Urasa, W. J. Mavura, V. D. Lewis and S. H. Nam " The Speciation of Manganese, Phosphorus and Platinum in Aqueous Solutions by using Ion Chromatography coupled with an Element Selective Detector." J. Chromatogr. **1991**, 547, 211-223.

I. T. Urasa and W. J. Mavura, " The Influence of Sample Acidification on the Speciation of Iron(II) and Iron(III)." Inter. J. Environ. Anal. Chem. **1992**, 48, 229-240.

W. J. Mavura and G. L. Long " Effect of a surfactant, on Emission Intensity of Slurry Injected Samples in Inductively Coupled Plasma Atomic Emission Spectrometry", submitted to *Appl. Spectrosc.* January **1994**

W. J. Mavura and G. L. Long " Temperature Measurements in Mixed Gases Inductively Coupled Plasma: Comparison between Cooling and Injector Gas Mixing." To be submitted to *Spectrochim. Acta B.*

Books

1. G. L. Long, W.J. Mavura, E. Lancaster, and G.R. Ducatte, "Alternative Methods of Sample Introduction for Plasma Emission Spectrometry," Virginia Water Resources Research Center, Blacksburg, VA, in press.

Presentations

W. J. Mavura and I. T. Urasa " Determination of the Distribution of Trace Metals in Soils and Sediments using Ion Chromatography Method coupled with a Spectroscopic Method." Sixty seventh Annual Meeting of Virginia Academy of Science, Richmond, VA May 1989, Paper 12.

W. J. Mavura "Application of Surfactants and Mixed Gas Inductively Coupled Plasma for the Determination of Metals Using Slurry Injection Technique."Presented at the Twenty first Annual Conference of the National Organization for the advancement of Black Chemists and Chemical Engineers (NOBCChE), in Atlantic City, New Jersey, April 1994.

W. J. Mavura
8/12/94